

UNCLASSIFIED

AD NUMBER

ADB016616

LIMITATION CHANGES

TO:

Approved for public release; distribution is unlimited.

FROM:

Distribution authorized to U.S. Gov't. agencies only; Test and Evaluation; FEB 1977. Other requests shall be referred to Air Force Armament Lab., Eglin AFB, FL.

AUTHORITY

AFATL ltr dtd 10 Apr 1980

THIS PAGE IS UNCLASSIFIED

AEDC-TR-77-8  
AFATL-TR-76-146

cy 2

OCT 08 1984



**AERODYNAMIC LOADS AND SEPARATION  
TRAJECTORIES FOR SEVERAL STORES  
WITH THE F-15 AIRCRAFT AT  
MACH NUMBERS FROM 0.6 TO 1.3**

**PROPULSION WIND TUNNEL FACILITY  
ARNOLD ENGINEERING DEVELOPMENT CENTER  
AIR FORCE SYSTEMS COMMAND  
ARNOLD AIR FORCE STATION, TENNESSEE 37389**

February 1977

**TECHNICAL REPORTS  
FILE COPY**

Final Report for Period August 9 through 18, 1976

This document has been approved for public release  
its distribution is unlimited. *per TAB 80-13*

Distribution limited to U. S. Government agencies only; this report contains information on test and evaluation of military hardware, February 1977; other requests for this document must be referred to Air Force Armament Laboratory (AFATL/DLJC), Eglin Air Force Base, Florida 32542.

Property of U. S. Air Force  
1 1 1 1 1 1  
1 1 1 1 1 1 1 1 1 1

Prepared for

**AIR FORCE ARMAMENT LABORATORY (AFATL/DLJC)  
EGLIN AIR FORCE BASE, FLORIDA 32542**

## NOTICES

When U. S. Government drawings specifications, or other data are used for any purpose other than a definitely related Government procurement operation, the Government thereby incurs no responsibility nor any obligation whatsoever, and the fact that the Government may have formulated, furnished, or in any way supplied the said drawings, specifications, or other data, is not to be regarded by implication or otherwise, or in any manner licensing the holder or any other person or corporation, or conveying any rights or permission to manufacture, use, or sell any patented invention that may in any way be related thereto.

Qualified users may obtain copies of this report from the Defense Documentation Center.

References to named commercial products in this report are not to be considered in any sense as an endorsement of the product by the United States Air Force or the Government.

## APPROVAL STATEMENT

This technical report has been reviewed and is approved for publication.

FOR THE COMMANDER



JOHN C. CARDOSI  
Lt Colonel, USAF  
Chief Air Force Test Director, PWT  
Directorate of Test



ALAN L. DEVEREAUX  
Colonel, USAF  
Director of Test

# UNCLASSIFIED

REPORT DOCUMENTATION PAGE		READ INSTRUCTIONS BEFORE COMPLETING FORM
<b>1 REPORT NUMBER</b> AEDC-TR-77-8 AFATL-TR-76-146	<b>2. GOVT ACCESSION NO.</b>	<b>3 RECIPIENT'S CATALOG NUMBER</b>
<b>4 TITLE (and Subtitle)</b> AERODYNAMIC LOADS AND SEPARATION TRAJECTORIES FOR SEVERAL STORES WITH THE F-15 AIRCRAFT AT MACH NUMBERS FROM 0.6 TO 1.3		<b>5 TYPE OF REPORT &amp; PERIOD COVERED</b> Final Report - August 9 - 18, 1976
<b>7. AUTHOR(s)</b>  George M. Kiber, ARO, Inc.		<b>6 PERFORMING ORG REPORT NUMBER</b>  <b>8 CONTRACT OR GRANT NUMBER(s)</b>
<b>9 PERFORMING ORGANIZATION NAME AND ADDRESS</b> Arnold Engineering Development Center (XO) Air Force Systems Command Arnold Air Force Station, Tennessee 37389		<b>10. PROGRAM ELEMENT, PROJECT TASK AREA &amp; WORK UNIT NUMBERS</b> Program Element 62602F Project 2567 Task 01
<b>11 CONTROLLING OFFICE NAME AND ADDRESS</b> Air Force Armament Laboratory (AFATL/DLJC) Eglin Air Force Base, Florida 32542		<b>12 REPORT DATE</b> February 1977
<b>14 MONITORING AGENCY NAME &amp; ADDRESS (if different from Controlling Office)</b>		<b>13 NUMBER OF PAGES</b> 71
		<b>15 SECURITY CLASS. (of this report)</b>  UNCLASSIFIED
		<b>15a DECLASSIFICATION/DOWNGRADING SCHEDULE</b> N/A
<b>16 DISTRIBUTION STATEMENT (of this Report)</b> Distribution limited to U. S. Government agencies only; this report contains information on test and evaluation of military hardware; February 1977; other requests for this document must be referred to Air Force Armament Laboratory (AFATL/DLJC), Eglin Air Force Base, Florida 32542.		
<b>17 DISTRIBUTION STATEMENT (of the abstract entered in Block 20, if different from Report)</b>		
<b>18 SUPPLEMENTARY NOTES</b>  Available in DDC		
<b>19 KEY WORDS (Continue on reverse side if necessary and identify by block number)</b> external stores                      separation                      F-15 aircraft aerodynamic loading                      trajectories                      captive tests aerodynamic characteristics                      transonic flow                      wind tunnel tests		
<b>20 ABSTRACT (Continue on reverse side if necessary and identify by block number)</b> A wind tunnel test was conducted at Mach numbers from 0.6 to 1.3 with 0.05-scale models of six stores and the F-15 aircraft. Extensive aerodynamic loads measurements were obtained for these stores in the aircraft flow field from the carriage position to 20 ft below the inboard pylon surfaces, with the majority of the data taken near the right-wing pylon. Aircraft angle of attack was varied from 0 to 10 deg. Separation trajectories were obtained for three of the stores at simulated altitudes from 5,000 to 18,000 ft at an aircraft angle of attack of 0.5 deg. Free-stream characteristics		

# UNCLASSIFIED

## 20. ABSTRACT (Continued)

for all stores were obtained with the aircraft model removed from the tunnel.

# UNCLASSIFIED

## PREFACE

The work reported herein was conducted by the Arnold Engineering Development Center (AEDC), Air Force Systems Command (AFSC), at the request of the Air Force Armament Laboratory (AFATL/DLJC), under Program Element 62602F. The Air Force Project Monitor was Capt. Robert Cason. The results of the test were obtained by ARO, Inc. (a subsidiary of Sverdrup Corporation), contract operator of AEDC, AFSC, Arnold Air Force Station, Tennessee, under ARO Project No. P41C-F3A. The author of this report was George M. Kiber, ARO, Inc. The data analysis was completed on October 4, 1976, and the manuscript (ARO Control No. ARO-PWT-TR-76-138) was submitted for publication on November 30, 1976.

## CONTENTS

	<u>Page</u>
1.0 INTRODUCTION . . . . .	7
2.0 APPARATUS	
2.1 Test Facility . . . . .	7
2.2 Test Articles . . . . .	8
2.3 Instrumentation . . . . .	8
3.0 TEST DESCRIPTION	
3.1 Test Conditions . . . . .	8
3.2 Data Acquisition . . . . .	9
3.3 Corrections . . . . .	10
3.4 Precision of Data . . . . .	10
4.0 RESULTS AND DISCUSSION	
4.1 Free-Stream Aerodynamic Data . . . . .	11
4.2 Aerodynamic Loads Data . . . . .	12
4.3 Separation Trajectories . . . . .	13

## ILLUSTRATIONS

### Figure

1. Isometric Drawing of a Typical Store Separation Installation and a Block Diagram of the Computer Control Loop . . . . .	15
2. Schematic of the Tunnel Test Section Showing Model Location . . . . .	16
3. Sketch of the F-15 Aircraft Model . . . . .	17
4. Details of the GBU-15 CWW Model . . . . .	18
5. Details of the GBU-15 PWV Model . . . . .	19
6. Details of the GBU-8 Model . . . . .	20
7. Details of the GBU-10 Model . . . . .	21
8. Details of the MK-84 LDGP Model . . . . .	22
9. Details of the BLU-27B/B(U) Model . . . . .	23
10. Details of the AIM-7 Missile Model . . . . .	24
11. Details of the F-15 Aircraft Inboard Pylon Model . . . . .	25
12. Sketch of the AIM-9 Missile and Launcher Models for the Inboard Pylon . . . . .	26

<u>Figure</u>	<u>Page</u>
13. Tunnel Installation Photograph Showing Aircraft, Store, and Captive Trajectory Support . . . . .	27
14. Free-Stream Characteristics of the GBU-15 CWW at Various Roll Angles . . . . .	28
15. Free-Stream Characteristics of the GBU-15 CWW at Various Yaw Angles . . . . .	31
16. Aerodynamic Characteristics of the GBU-15 CWW at Various Orientations Relative to the Carriage Position . . . . .	34
17. Delta-Coefficient Data for the GBU-15 CWW at Various Orientations Relative to the Carriage Position . . . . .	36
18. Aerodynamic Characteristics Showing the Effects of Varying Longitudinal Position at Constant Lateral Positions . . . . .	38
19. Aerodynamic Characteristics Showing the Effects of Varying Lateral Position at Constant Longitudinal Positions . . . . .	41
20. Delta-Coefficient Data for Varying Longitudinal and Constant Lateral Positions . . . . .	44
21. Delta-Coefficient Data for Varying Lateral and Constant Longitudinal Positions . . . . .	47
22. Effects of the AIM-9 Missiles and Launchers on the Aerodynamic Characteristics of the MK-84 LDGP . . . . .	50
23. Separation Characteristics of the GBU-10 from the F-15 Aircraft . . . . .	55
24. Separation Characteristics of the MK-84 LDGP from the F-15 Aircraft . . . . .	57
25. Separation Characteristics of the BLU-27B/B(U) from the F-15 Aircraft . . . . .	59

**TABLES**

1. Test Summary-Aerodynamic Loads . . . . .	61
2. Test Summary-Separation Trajectories . . . . .	64

<u>Table</u>	<u>Page</u>
3. Full-Scale Store Parameters Used in Trajectory Calculations . . . . .	65
4. Aircraft Loading Configurations . . . . .	66
NOMENCLATURE . . . . .	67

## 1.0 INTRODUCTION

A wind tunnel investigation was conducted using 0.05-scale models of six stores and the F-15 aircraft. The test results, which will be used to validate assumptions made in conducting abbreviated array tests, consisted of aerodynamic characteristics of the stores in the aircraft flow field, separation trajectories for certain stores from the aircraft, and free-stream aerodynamic characteristics for the stores. The data were obtained using a six-degree-of-freedom captive trajectory support (CTS) store-separation system. The test was conducted at Mach numbers from 0.6 to 1.3 in the Aerodynamic Wind Tunnel (4T) of the Propulsion Wind Tunnel Facility (PWT).

## 2.0 APPARATUS

### 2.1 TEST FACILITY

The Aerodynamic Wind Tunnel (4T) is a closed-loop, continuous flow, variable-density tunnel in which the Mach number can be varied from 0.1 to 1.3. At all Mach numbers, the stagnation pressure can be varied from 300 to 3,700 psfa. The test section is 4 ft square and 12.5 ft long with perforated, variable porosity (0.5- to 10-percent open) walls. It is completely enclosed in a plenum chamber from which the air can be evacuated, allowing part of the tunnel airflow to be removed through the perforated walls of the test section.

For store separation testing, two separate and independent support systems are used to support the models. The aircraft model is inverted in the test section and supported by an offset sting attached to the main pitch sector. The store model is supported by the CTS which extends down from the tunnel top wall and provides store movement (six degrees of freedom) independent of the aircraft model. An isometric drawing of a typical store separation installation is shown in Fig. 1.

Also shown in Fig. 1 is a block diagram of the computer control loop used during captive trajectory testing. The analog system and the digital computer work as an integrated unit and, utilizing required input information, control the store movement during a trajectory. Store positioning is accomplished by use of six individual d-c electric motors. Maximum translational travel of the CTS is  $\pm 15$  in. from the tunnel centerline in the lateral and vertical directions and 36 in. in the axial direction. Maximum angular displacements are  $\pm 45$  deg in pitch and yaw and  $\pm 360$  deg in roll.

description of the test facility can be found in the Test Facilities Handbook.<sup>1</sup> A schematic showing the test section details and the location of the models in the tunnel is shown in Fig. 2.

## 2.2 TEST ARTICLES

During the test, 0.05-scale models of the F-15 aircraft and various stores were used. The stores tested included (1) GBU-15 CWW, (2) GBU-15 PWW, (3) GBU-8, (4) GBU-10, (5) MK-84 LDGP, and (6) BLU-27B/B(U). Basic details and dimensions of the F-15 aircraft model and the store models are presented in Figs. 3 and 4 through 9, respectively. The aircraft model was configured with AIM-7 missiles (Fig. 10) on all four fuselage stations, and was geometrically similar to the full-scale aircraft except that the horizontal tail surfaces were removed to minimize interference with the CTS movement. The F-15 aircraft model had both inboard pylons (Fig. 11) installed and rigged for CTS testing. The left-wing inboard pylon was configured with AIM-9 missiles and launchers as shown in Fig. 12. A typical tunnel installation photograph, showing the aircraft, store model, and CTS is presented in Fig. 13.

## 2.3 INSTRUMENTATION

A six-component internal strain-gage balance was used to obtain store aerodynamic force and moment data. Translational and angular positions of the stores were obtained from CTS analog inputs during separation trajectories and from digital computer commands during aerodynamic testing. The F-15 aircraft-model angle of attack was determined using an internal, gravimetric, angular position indicator. The inboard pylon surfaces each contained an infrared optical sensor to provide an indication of when the store was at the carriage position. The system was also electrically connected to automatically stop the CTS movement if the store model or sting support contacted the aircraft model or its support structure.

## 3.0 TEST DESCRIPTION

### 3.1 TEST CONDITIONS

Separation trajectory, aerodynamic loads, and free-stream data were obtained at Mach numbers from 0.6 to 1.3. Tunnel dynamic pressure ranged from 315 psf at  $M_\infty =$

---

<sup>1</sup>Test Facilities Handbook (Tenth Edition). "Propulsion Wind Tunnel Facility, Vol. 4." Arnold Engineering Development Center, May 1974.

0.6 to 511 psf at  $M_\infty = 1.3$ , and tunnel stagnation temperature was maintained near 100°F. A complete test summary and the wind tunnel nominal test conditions are given in Tables 1 and 2.

Tunnel conditions were held constant at the desired Mach number and stagnation pressure while data were obtained. The trajectories were terminated when the store or sting contacted the aircraft model or when a CTS limit was reached.

## 3.2 DATA ACQUISITION

### 3.2.1 Trajectory Data

To obtain a trajectory, test conditions were established in the tunnel and the aircraft model was positioned at the desired angle of attack. The store model was then oriented to a position corresponding to the store carriage location. After the store was set at the desired initial position, operational control of the CTS was switched to the digital computer which controlled the store movement during the trajectory through commands to the CTS analog system (see block diagram, Fig. 1). Data from the wind tunnel, consisting of measured model forces and moments, wind tunnel operating conditions, and CTS rig positions, were input to the digital computer for use in the full-scale trajectory calculations.

The digital computer was programmed to solve the six-degree-of-freedom equations to calculate the angular and linear displacements of the store relative to the aircraft. In general, the program involves using the last two successively measured values of each static aerodynamic coefficient to predict the magnitude of the coefficients over the next time interval of the trajectory. These predicted values are used to calculate the new position and attitude of the store at the end of the time interval. The CTS is then commanded to move the store model to this new position, and the aerodynamic loads are measured. If these new measurements agree with the predicted values, the process is continued over another time interval of the same magnitude. If the measured and predicted values do not agree within the desired precision, the calculation is repeated over a time interval one-half the previous value. This process is repeated until a complete trajectory has been obtained.

In applying the wind tunnel data to the calculations of the full-scale store trajectories, the measured forces and moments are reduced to coefficient form and then applied with proper full-scale store dimensions and flight dynamic pressure. Dynamic pressure was calculated using a flight velocity equal to the free-stream velocity component plus the components of store velocity relative to the aircraft, and a density corresponding to the simulated altitude.

The initial portion of each launch trajectory incorporated simulated ejector forces in addition to the measured aerodynamic forces acting on the store. The ejector force values used for the stores are presented in Table 2. The ejector force was considered to act perpendicularly to the pylon-mounting surface. The locations of the applied ejector forces and other full-scale store parameters used in the trajectory calculations are listed in Table 3.

### 3.2.2 Aerodynamic Loads Data

Store aerodynamic data in the free stream and in the aircraft flow field were obtained in the following manner. After tunnel conditions were established and the aircraft-model angle of attack was set (when applicable), operational control of the CTS was switched to the digital computer. The computer then positioned the store at  $\alpha_s = 0$  (free-stream data) or at a known location with respect to the parent aircraft (flow-field data) through commands to the CTS (see block diagram, Fig. 1). After initial-point data were recorded, the digital computer then positioned the store at preselected orientations and center-of-gravity (cg) positions programmed into the computer. At each set position, the wind tunnel operating conditions and the store model forces and moments were measured and recorded. The model aerodynamic loads were then reduced to coefficient form and tabulated point by point by the digital computer.

### 3.3 CORRECTIONS

Balance, sting, and support deflections caused by the aerodynamic loads on the store models were accounted for in the data reduction program to calculate the true store-model angles and positions. Corrections were also made for model weight tares to calculate the net aerodynamic forces on the store model.

### 3.4 PRECISION OF DATA

The estimated uncertainties in store-model positioning from the ability of the CTS to set on a specified value were  $\pm 0.10$  ft (full-scale equivalent) for translational settings and  $\pm 0.15$  deg in pitch and yaw. The estimated uncertainty in aircraft model angle of attack was  $\pm 0.1$  deg. The Mach number was held constant within  $\pm 0.005$  of the quoted Mach number with an estimated uncertainty of  $\pm 0.003$ .

### 3.4.1 Aerodynamic Loads

The balance uncertainties, based on a 95-percent confidence level, were combined with the uncertainties in the tunnel measurements to estimate the precision of the aerodynamic coefficients. The maximum estimated uncertainties are given as follows:

<u>Store</u>	<u><math>\Delta C_N</math></u>	<u><math>\Delta C_Y</math></u>	<u><math>\Delta C_A</math></u>	<u><math>\Delta C_m</math></u>	<u><math>\Delta C_n</math></u>	<u><math>\Delta C_l</math></u>
GBU-15 CWW	$\pm 0.02$	$\pm 0.02$	$\pm 0.01$	$\pm 0.02$	$\pm 0.02$	$\pm 0.01$
GBU-15 PWW	$\pm 0.02$	$\pm 0.02$	$\pm 0.01$	$\pm 0.02$	$\pm 0.02$	$\pm 0.01$
GBU-8	$\pm 0.02$	$\pm 0.02$	$\pm 0.01$	$\pm 0.02$	$\pm 0.02$	$\pm 0.01$
GBU-10	$\pm 0.01$					
MK-84 LDGP	$\pm 0.01$	$\pm 0.01$	$\pm 0.01$	$\pm 0.02$	$\pm 0.02$	$\pm 0.01$
BLU-27B/B(U)	$\pm 0.01$	$\pm 0.01$	$\pm 0.01$	$\pm 0.02$	$\pm 0.01$	$\pm 0.01$

### 3.4.2 Trajectory Data

The trajectory data are subject to error from several sources including tunnel conditions, balance measurements, extrapolation tolerances allowed in the predicted coefficients, computer inputs, and CTS positioning control. Extrapolation tolerances were  $\pm 0.10$  for the aerodynamic coefficients. The maximum estimated uncertainties in the full-scale position data caused by the balance precision limitations are as follows:

<u>Time, sec</u>	<u><math>\Delta X</math></u>	<u><math>\Delta Y</math></u>	<u><math>\Delta Z</math></u>	<u><math>\Delta \theta</math></u>	<u><math>\Delta \psi</math></u>	<u><math>\Delta \phi</math></u>
0.10	$\pm 0.004$	$\pm 0.003$	$\pm 0.003$	$\pm 0.07$	$\pm 0.05$	$\pm 0.63$
0.40	$\pm 0.020$	$\pm 0.016$	$\pm 0.015$	$\pm 0.39$	$\pm 0.30$	$\pm 6.30$

## 4.0 RESULTS AND DISCUSSION

Because of the large volume of data obtained during this test, only selected data are presented herein. A complete listing of all data obtained during the test is given in Tables 1 and 2. The aircraft loading configurations are defined in Table 4.

### 4.1 FREE-STREAM AERODYNAMIC DATA

Free-stream data were obtained for all stores over the angle ranges listed in Table 1. A portion of these data for the GBU-15 CWW is presented in Figs. 14 and 15. The

effects of model roll angle are shown in Fig. 14. The most significant effects are on the side-force, yawing-moment, and rolling-moment coefficients. Although exhibiting different characteristics, the same coefficients are affected in the yaw data presented in Fig. 15.

## 4.2 AERODYNAMIC LOADS DATA

Aerodynamic force and moment data for all stores were obtained at Mach numbers from 0.6 to 1.2. Store cg positions and angular orientations relative to the carriage position are presented in Table 1 along with a test summary.

Aerodynamic loads data for a vertical traverse of the GBU-15 CWW at various angular orientations relative to the carriage position are shown in Fig. 16. The data show that the pitching-moment and normal-force coefficients were primarily influenced by pitch angle, whereas the other coefficients remained relatively unchanged. The data obtained at various yaw angles relative to the carriage position show the side-force, yawing-moment, and pitching-moment coefficients were influenced by yaw angle. Presented in Fig. 17 are the delta-coefficient data which correspond to the data presented in Fig. 16. These delta-coefficients, or interference data, represent the difference between the store measured force and moment data, obtained in a particular orientation in the aircraft flow field, and the free-stream force and moment data for the store at the same orientation. As defined here, the delta-coefficients should have had a value of zero when the store was far enough away from the aircraft to be in the free stream. The data presented herein show only slight influence of the aircraft flow field at a vertical displacement of 20 ft, but significantly larger influences as the distance between the store and the pylon surface was decreased. These influences are also shown to be dependent on the store orientation.

Aerodynamic force and moment data as a function of vertical distance for various lateral and longitudinal positions relative to the carriage position are shown in Figs. 18 and 19. The effects of longitudinal (X) position at constant lateral (Y) position are shown in Fig. 18. The effects of lateral position for constant longitudinal position are shown in Fig. 19. The delta-coefficients corresponding to the longitudinal and lateral positions in Figs. 18 and 19 are presented in Figs. 20 and 21, respectively.

Data presented in Fig. 22 show the effect of the AIM-9 missiles and launchers on the normal-force and pitching-moment coefficients of the MK-84 LDGP store at various Mach numbers. The largest effects were on the pitching-moment coefficient. The change in sign on the yawing-moment coefficients was the effect of crossflow, since the two sets of data were obtained on opposite sides of the aircraft.

### 4.3 SEPARATION TRAJECTORIES

Separation trajectory data were obtained for the store configurations and flight conditions listed in Table 2. Data showing the linear displacements from the carriage position and angular displacements of the stores relative to the flight direction are presented in Figs. 23 through 25. The full-scale parameters used in the trajectory calculations are listed in Table 3. The effects of the AIM-9 missiles and launchers can be seen in the trajectories from the right and left wings obtained at identical flight conditions. The presence of these missiles tends to produce larger angular motions of the stores.

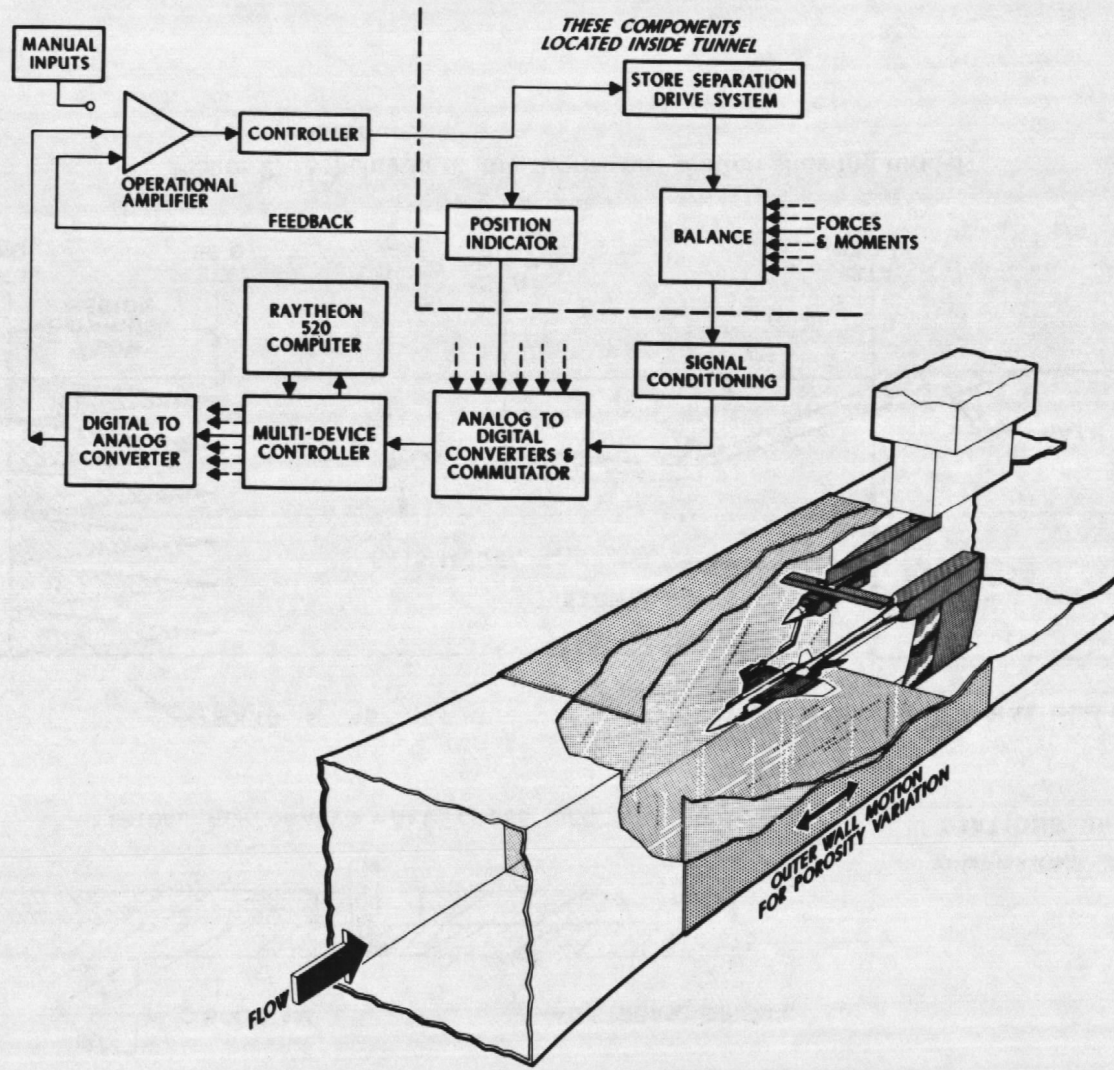


Figure 1. Isometric drawing of a typical store installation and block diagram of the computer control loop.

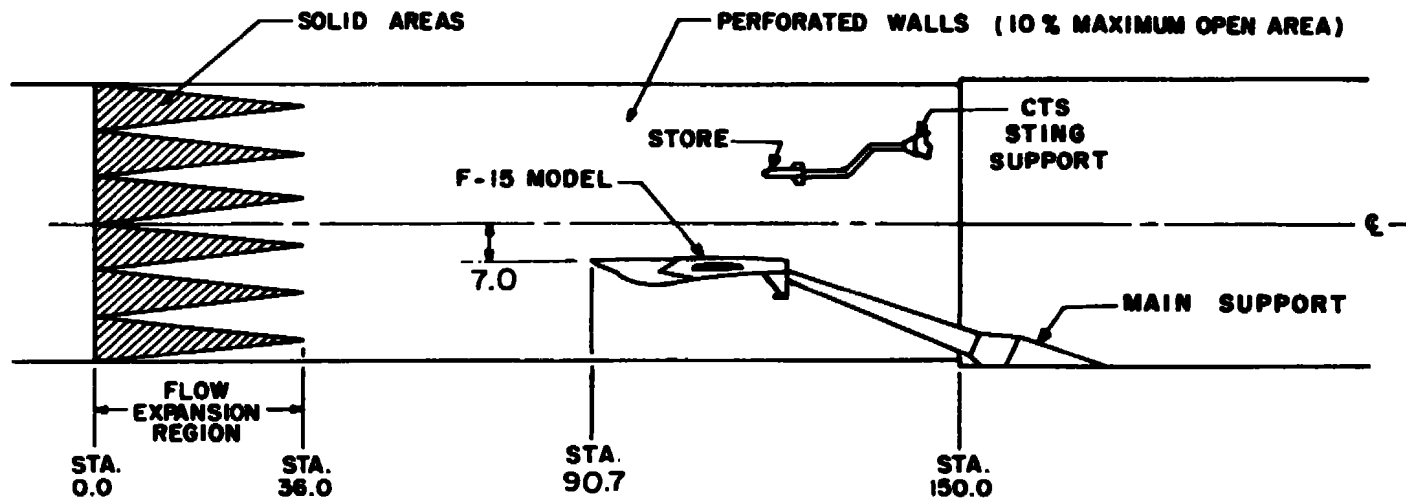
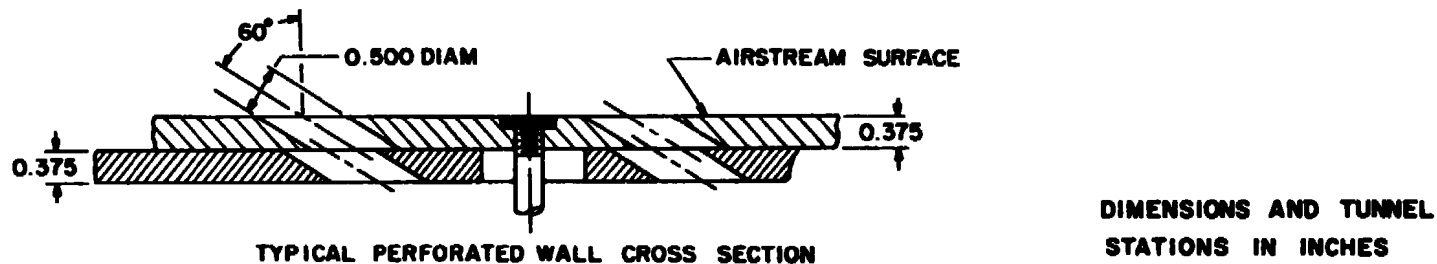


Figure 2. Schematic of the tunnel test section showing model location.

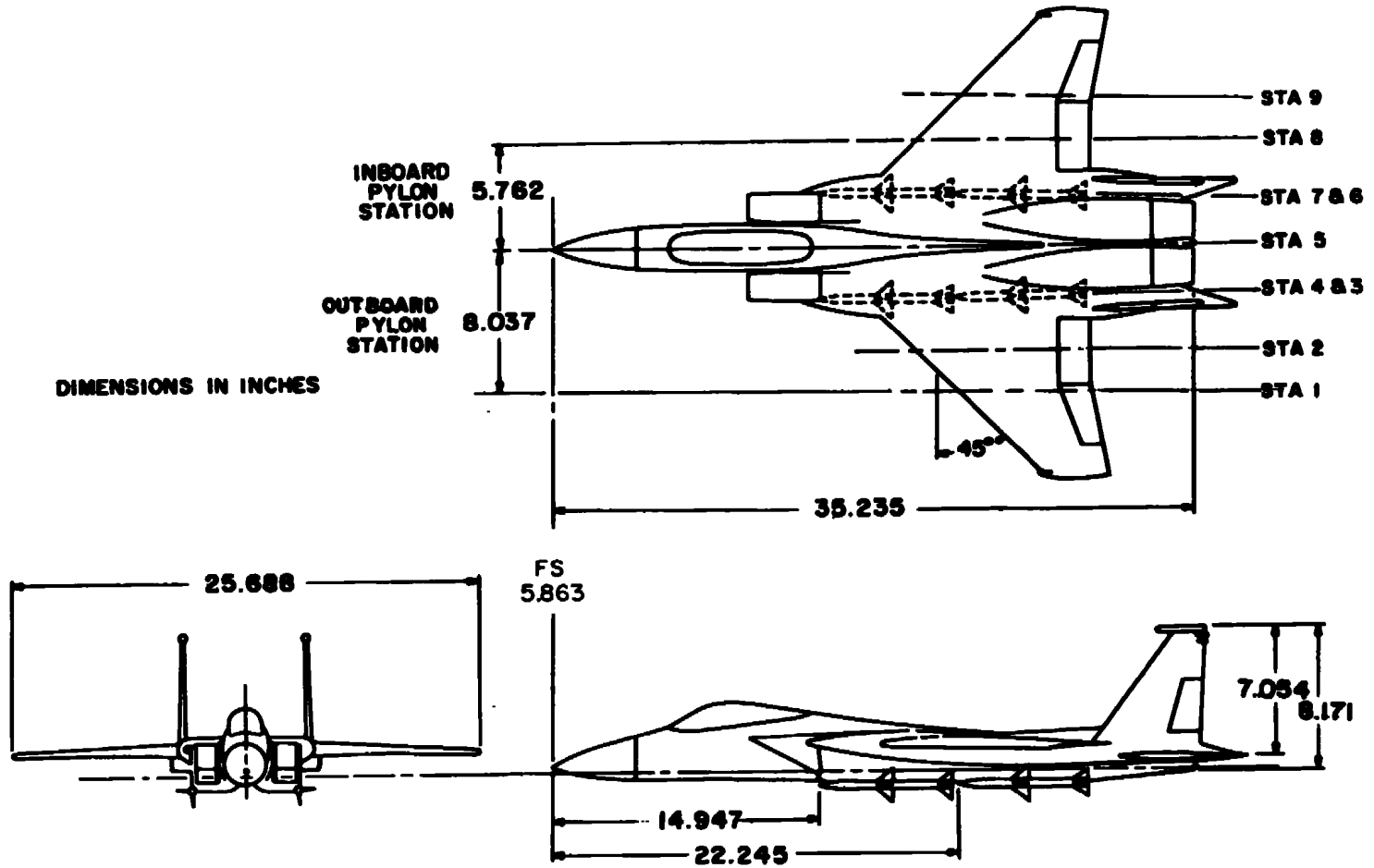
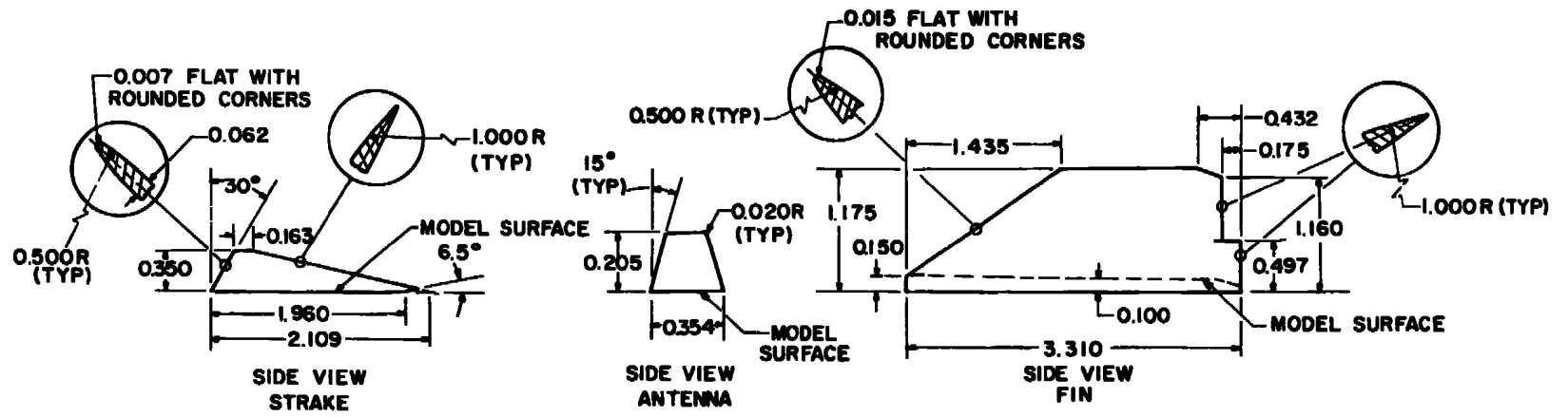


Figure 3. Sketch of the F-15 aircraft model.



18

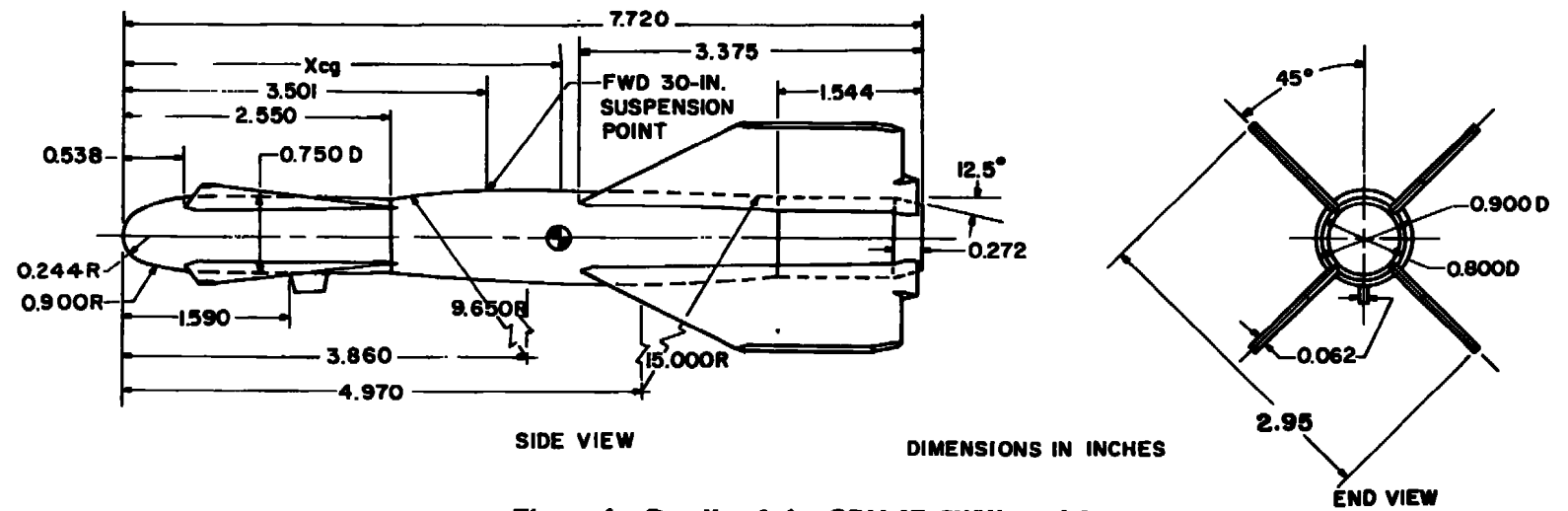


Figure 4. Details of the GBU-15 CWW model.

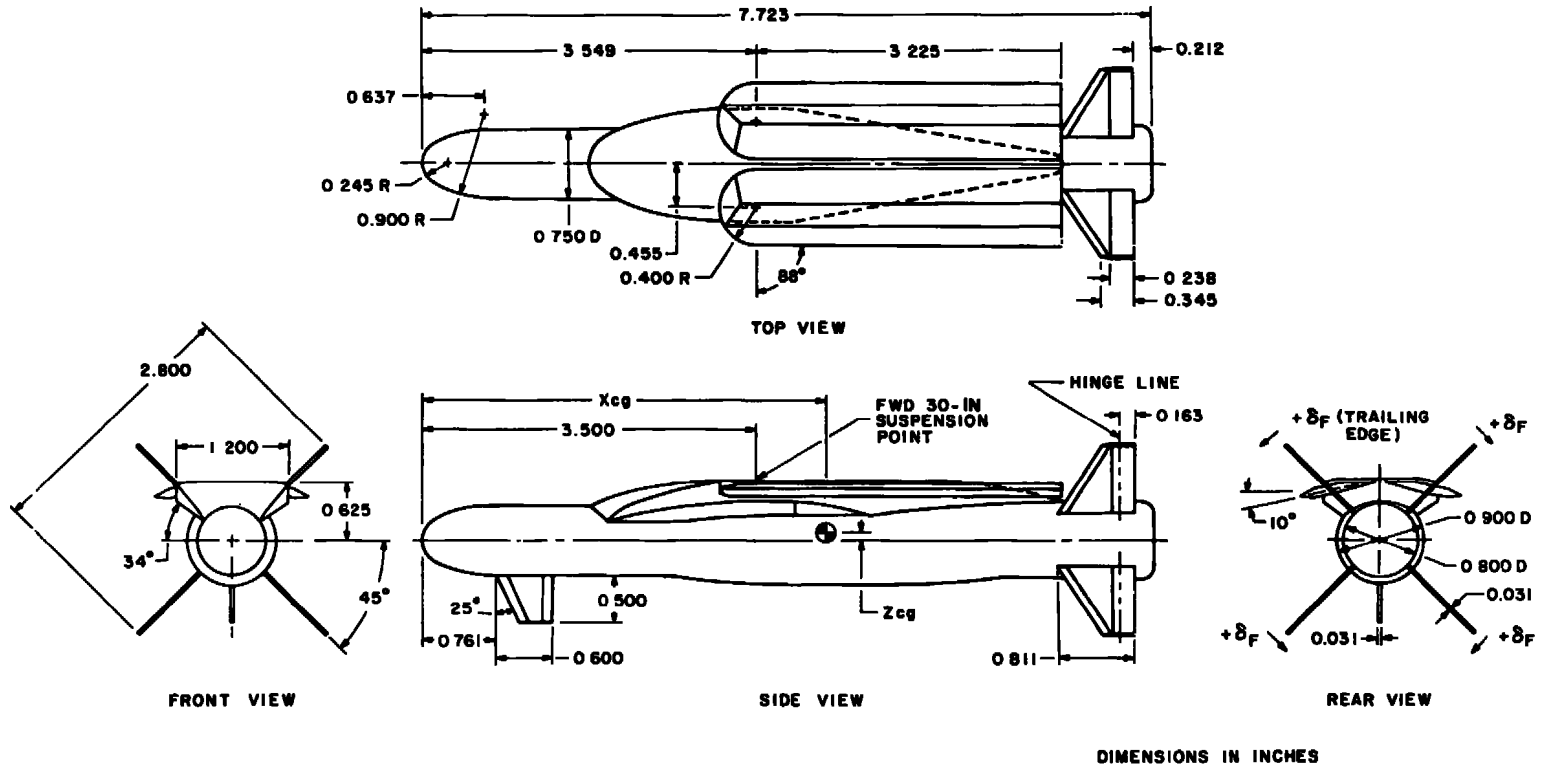
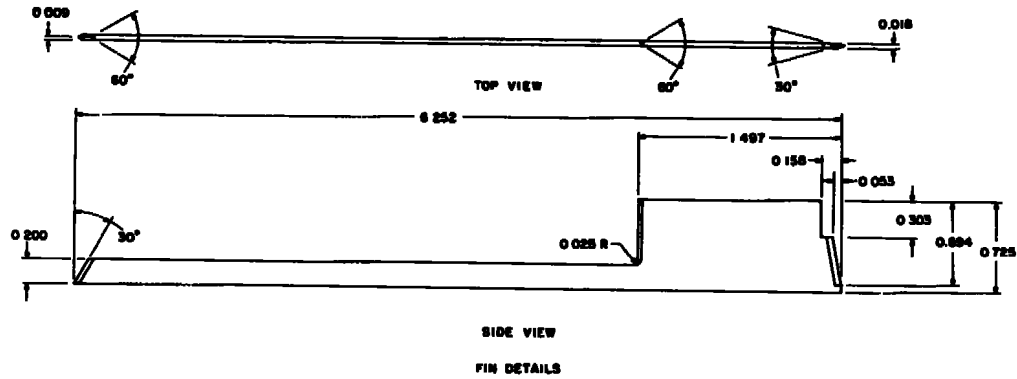


Figure 5. Details of the GBU-15 PWW model.



X, in	R, in
2.273	0.364
2.385	0.376
2.585	0.394
2.785	0.412
2.985	0.428
3.185	0.438
3.385	0.446
3.580	0.450
4.000	0.480
4.250	0.480
4.500	0.480
4.694	0.450
4.894	0.448
5.094	0.444
5.294	0.437
5.494	0.428
5.694	0.418
5.894	0.401
5.918	0.400

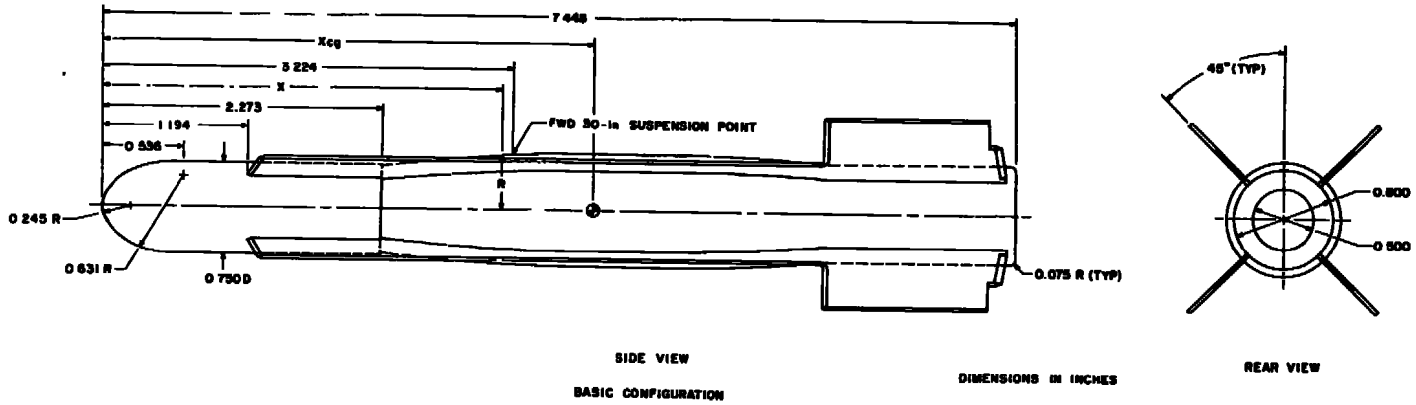
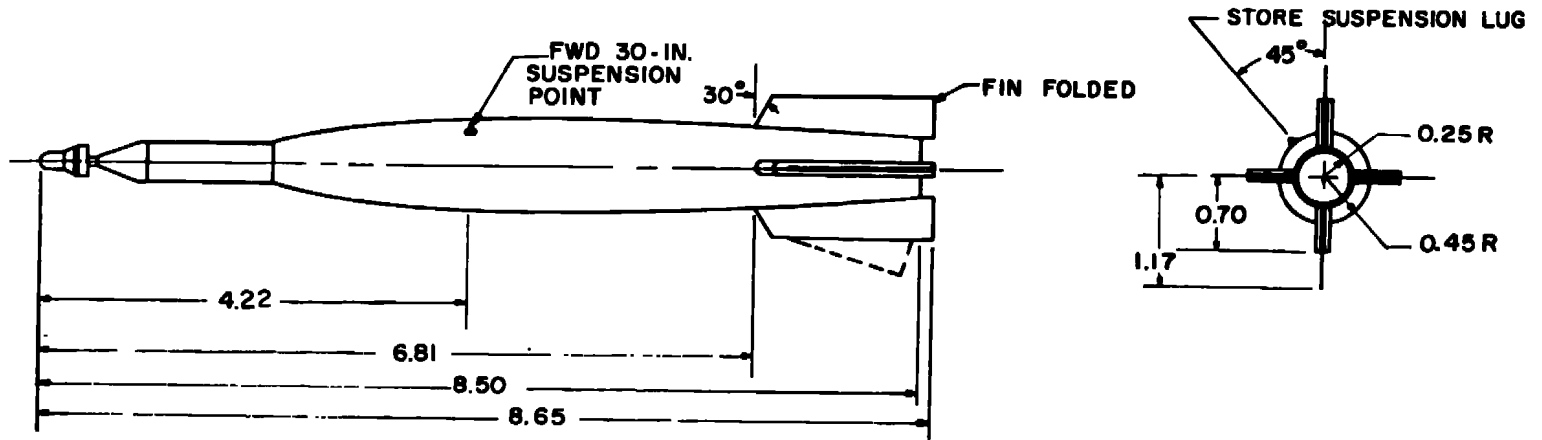


Figure 6. Details of the GBU-8 model.



MODEL SHOWN ROLLED -45°  
DIMENSIONS IN INCHES

Figure 7. Details of the GBU-10 model.

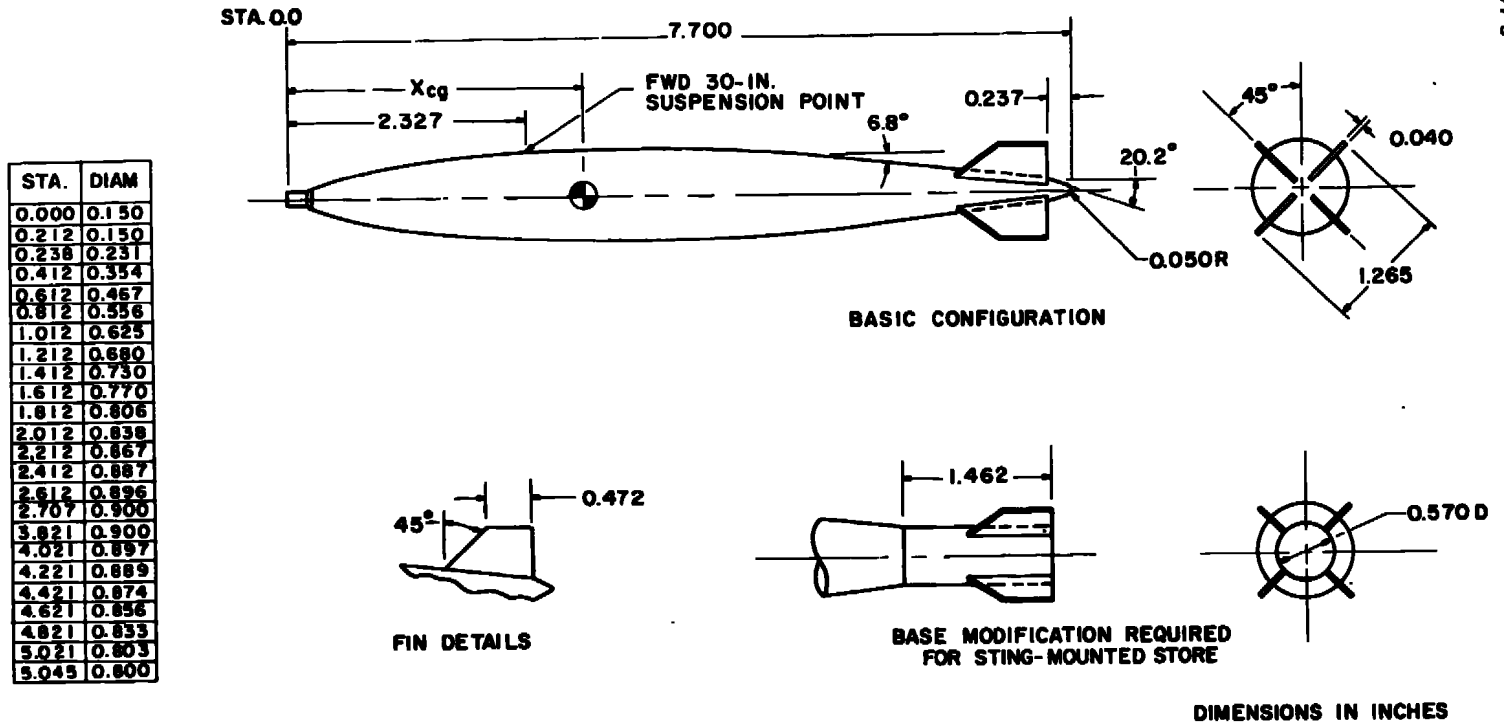


Figure 8. Details of the MK-84 LDGP model.

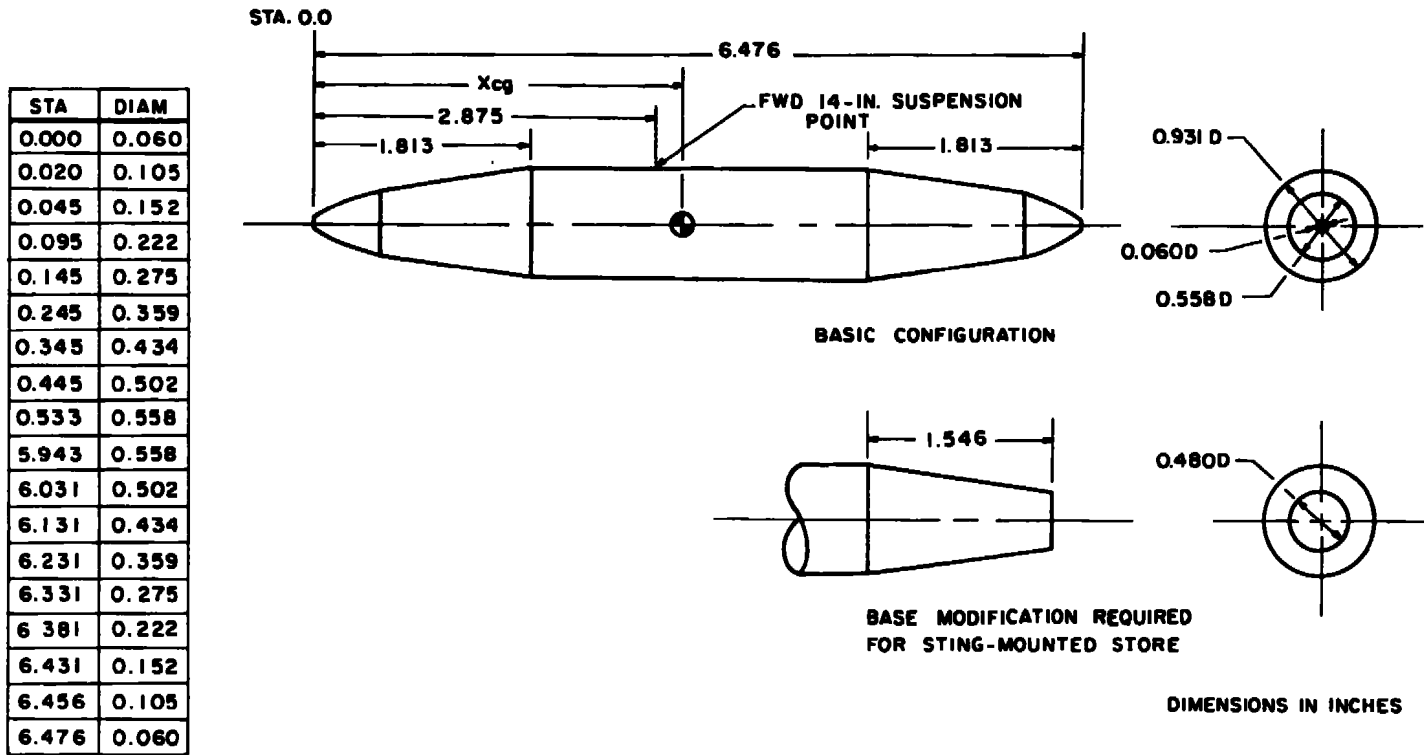
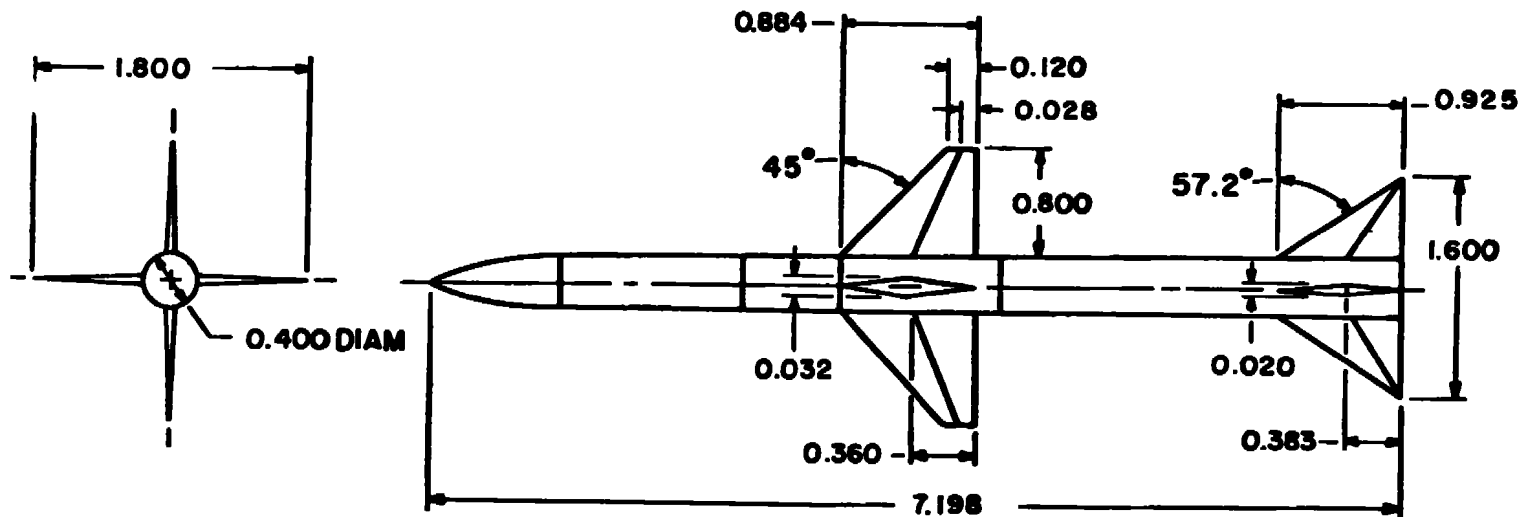
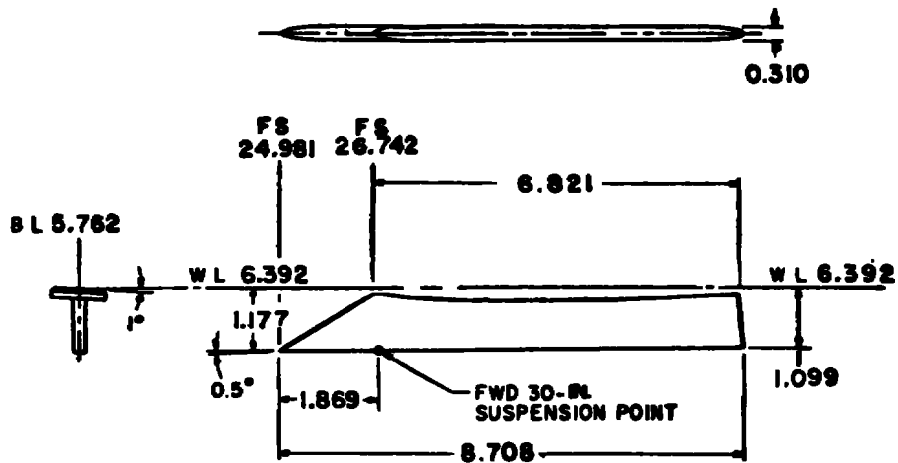


Figure 9. Details of the BLU-27B/B(U) model.



**DIMENSIONS IN INCHES**

**Figure 10. Details of the AIM-7 missile model.**



INBOARD WING PYLON

DIMENSIONS IN INCHES

Figure 11. Details of the F-15 aircraft inboard pylon model.

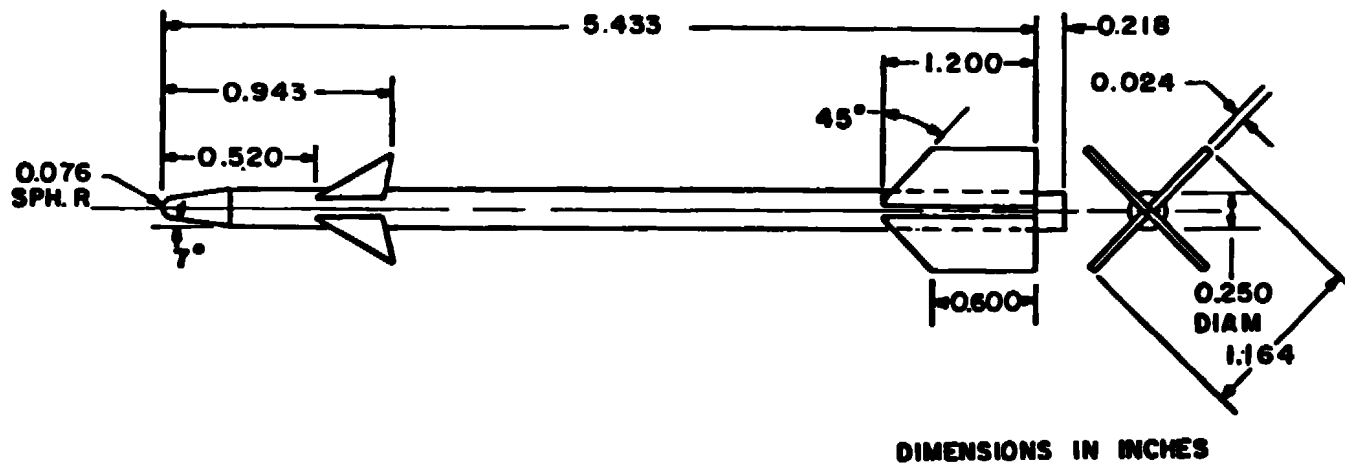
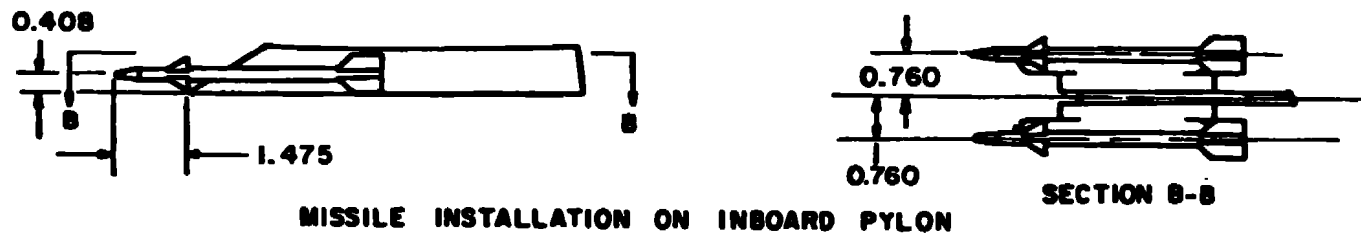
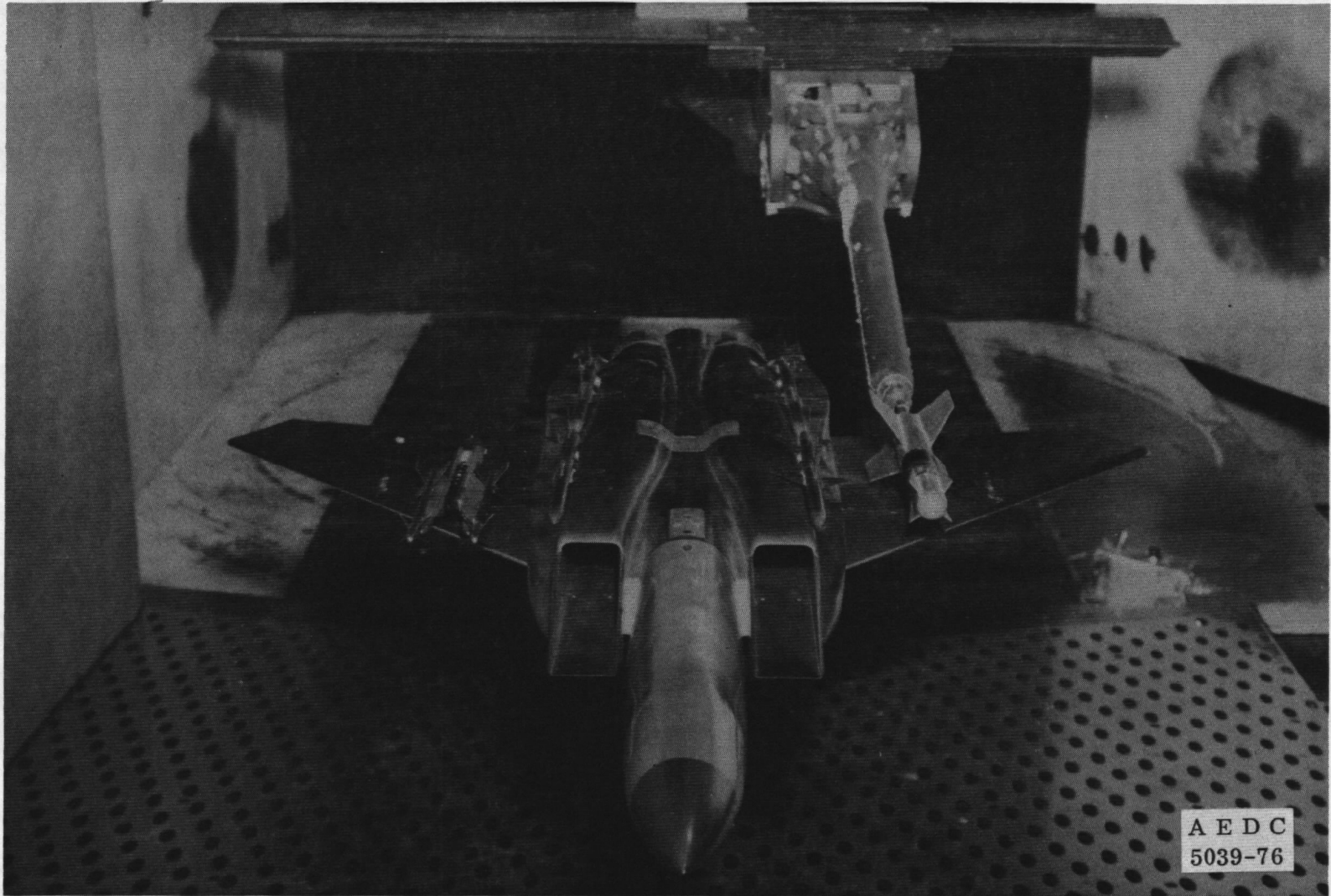
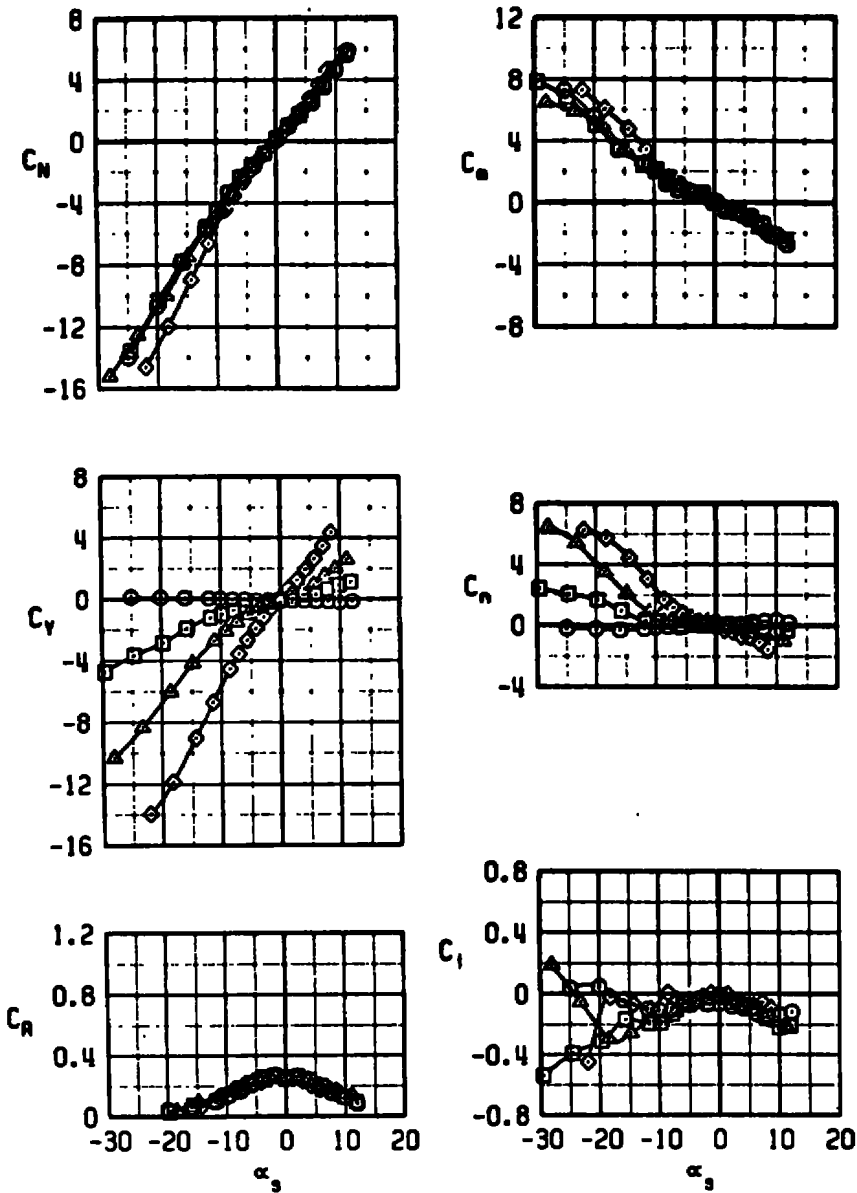


Figure 12. Sketch of the AIM-9 missile and launcher models for the inboard pylon.



**Figure 13. Tunnel installation photograph showing aircraft, store, and captive trajectory support.**

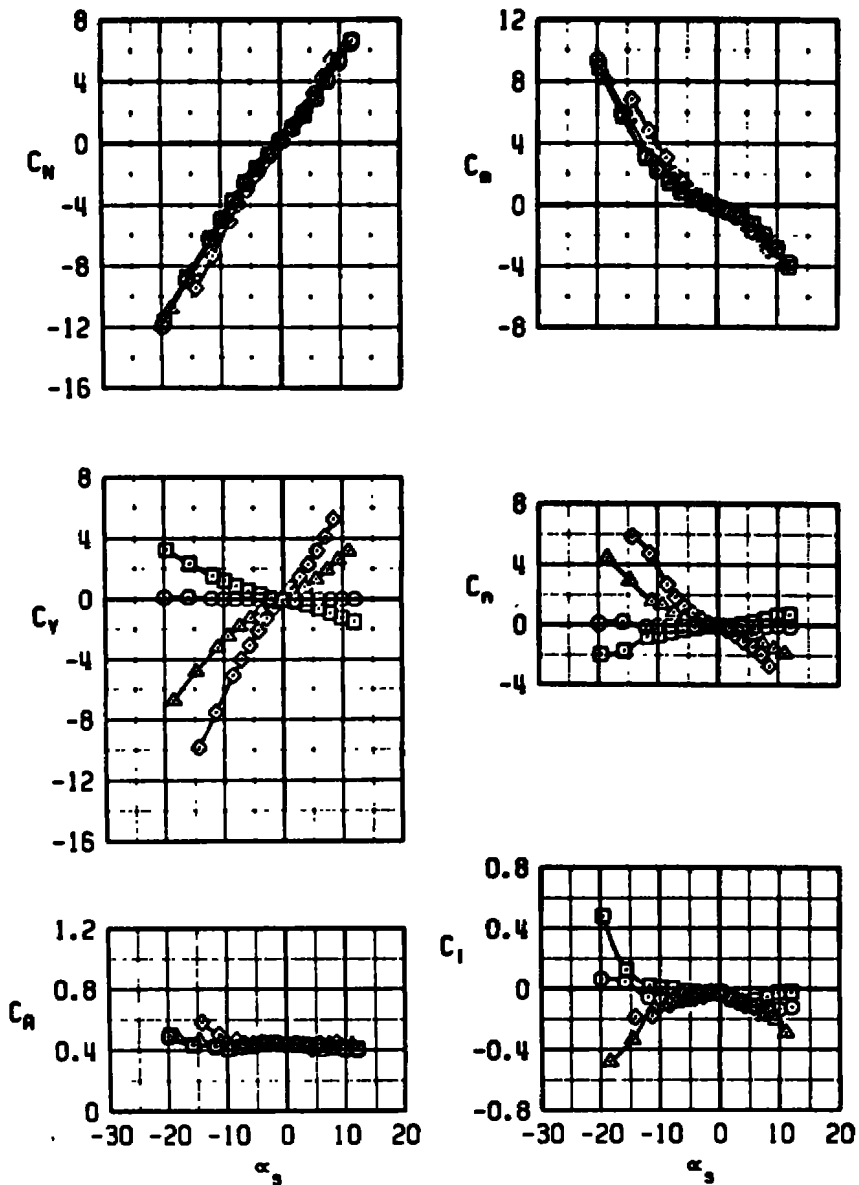
SYM	M <sub>∞</sub>	STORE	●
○	0.60	GBU-15 CWM	0
□	0.60	GBU-15 CWM	-10
△	0.60	GBU-15 CWM	-22.5
◇	0.60	GBU-15 CWM	-45



a.  $M_\infty = 0.6$

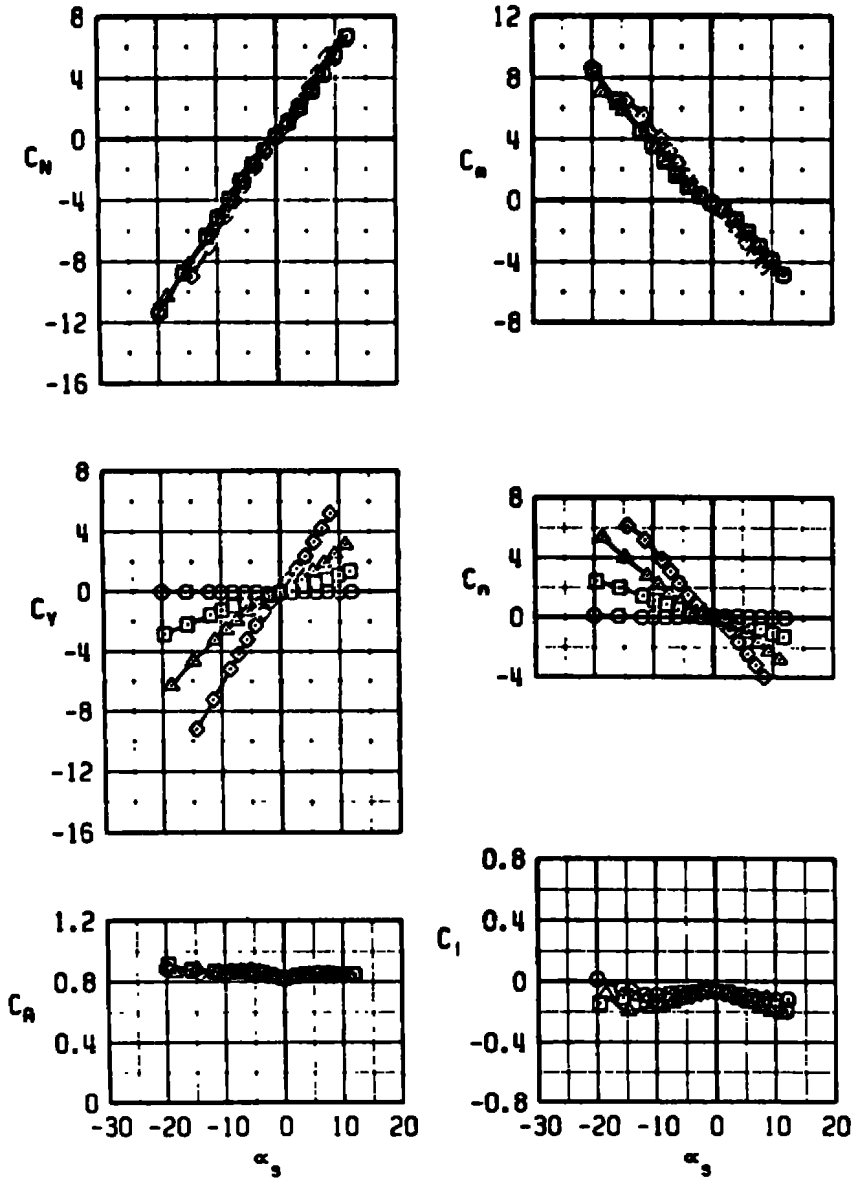
Figure 14. Free-stream characteristics of the GBU-15 CWW at various roll angles.

SYM	$M_\infty$	STORE	$\theta$
○	0.95	GBU-15 CMM	0
□	0.95	GBU-15 CMM	10
△	0.95	GBU-15 CMM	22.5
◇	0.95	GBU-15 CMM	45



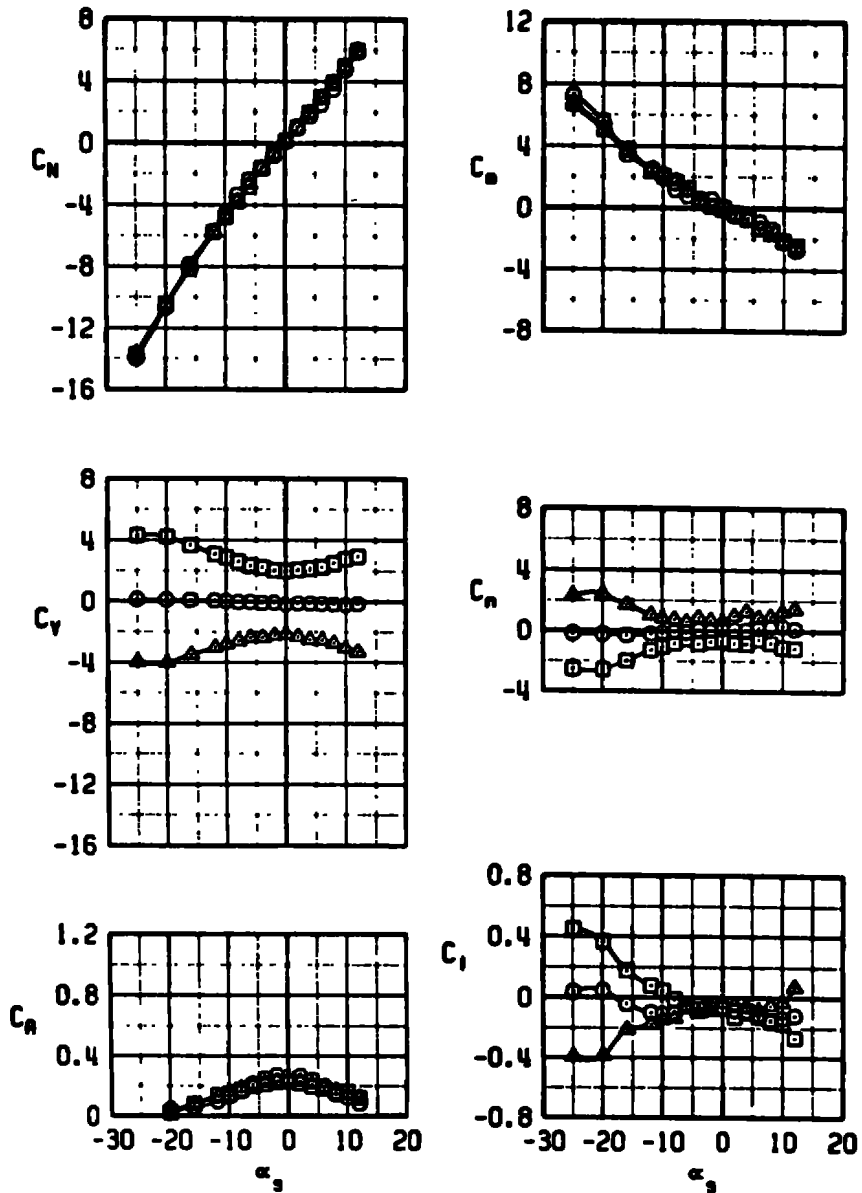
b.  $M_\infty = 0.95$   
 Figure 14. Continued.

SYM	M <sub>L</sub>	STORE	•
○	1.20	GBU-15 CMW	0
□	1.20	GBU-15 CMW	-10
△	1.20	GBU-15 CMW	-22.5
◇	1.20	GBU-15 CMW	-45



c.  $M_\infty = 1.20$   
 Figure 14. Concluded.

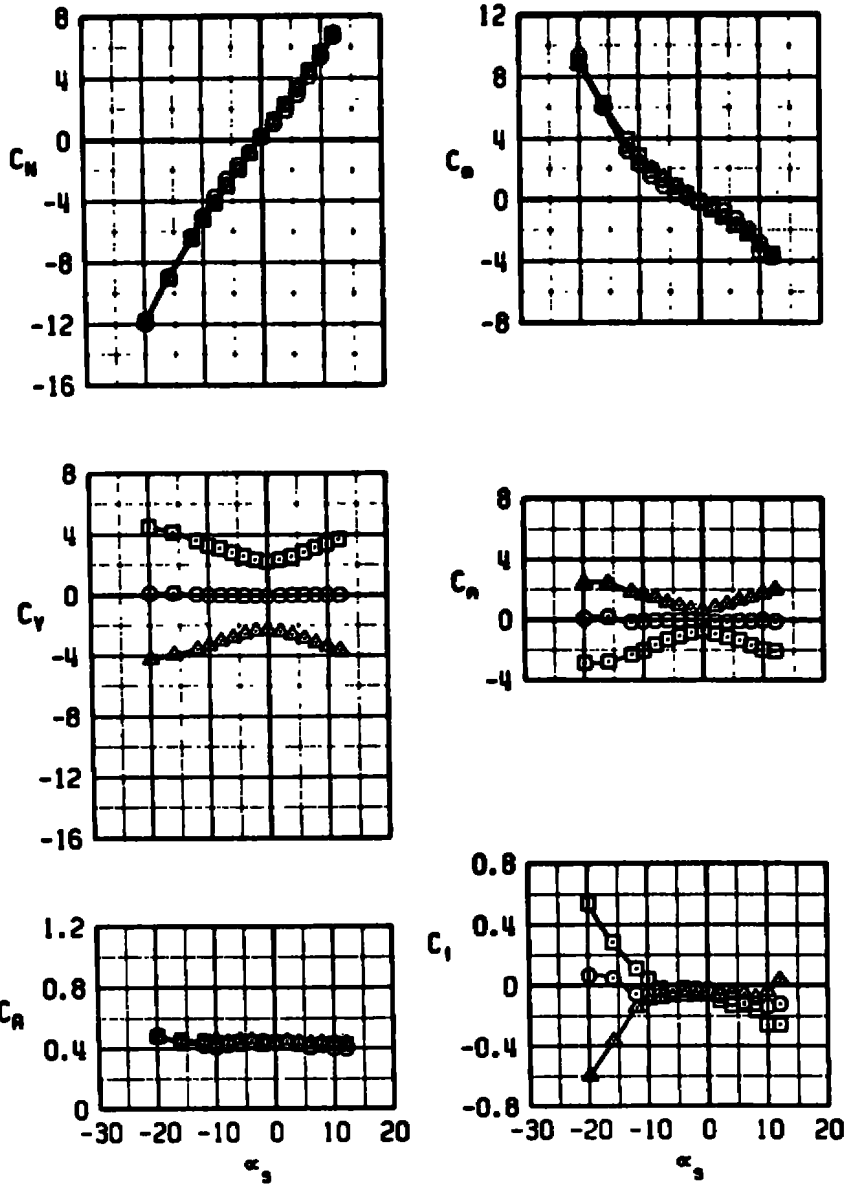
SYM	M <sub>∞</sub>	STORE	•
○	0.60	GBU-15 CWW	0
□	0.60	GBU-15 CWW	5
△	0.60	GBU-15 CWW	-5



a.  $M_\infty = 0.6$

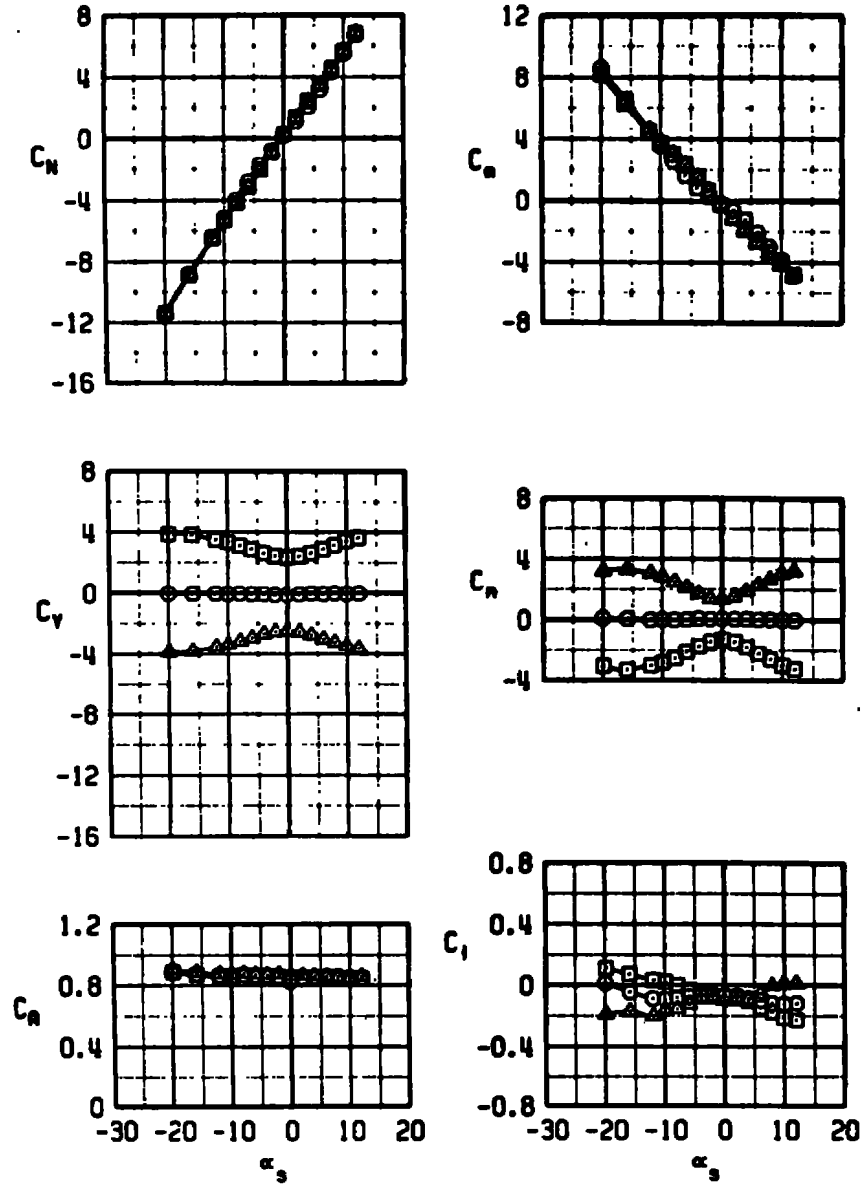
Figure 15. Free-stream characteristics of the GBU-15 CWW at various yaw angles.

SYM	$M_\infty$	STORE	$\delta$
○	0.95	GBU-15 CMN	0
□	0.95	GBU-15 CMN	5
△	0.95	GBU-15 CMN	-5



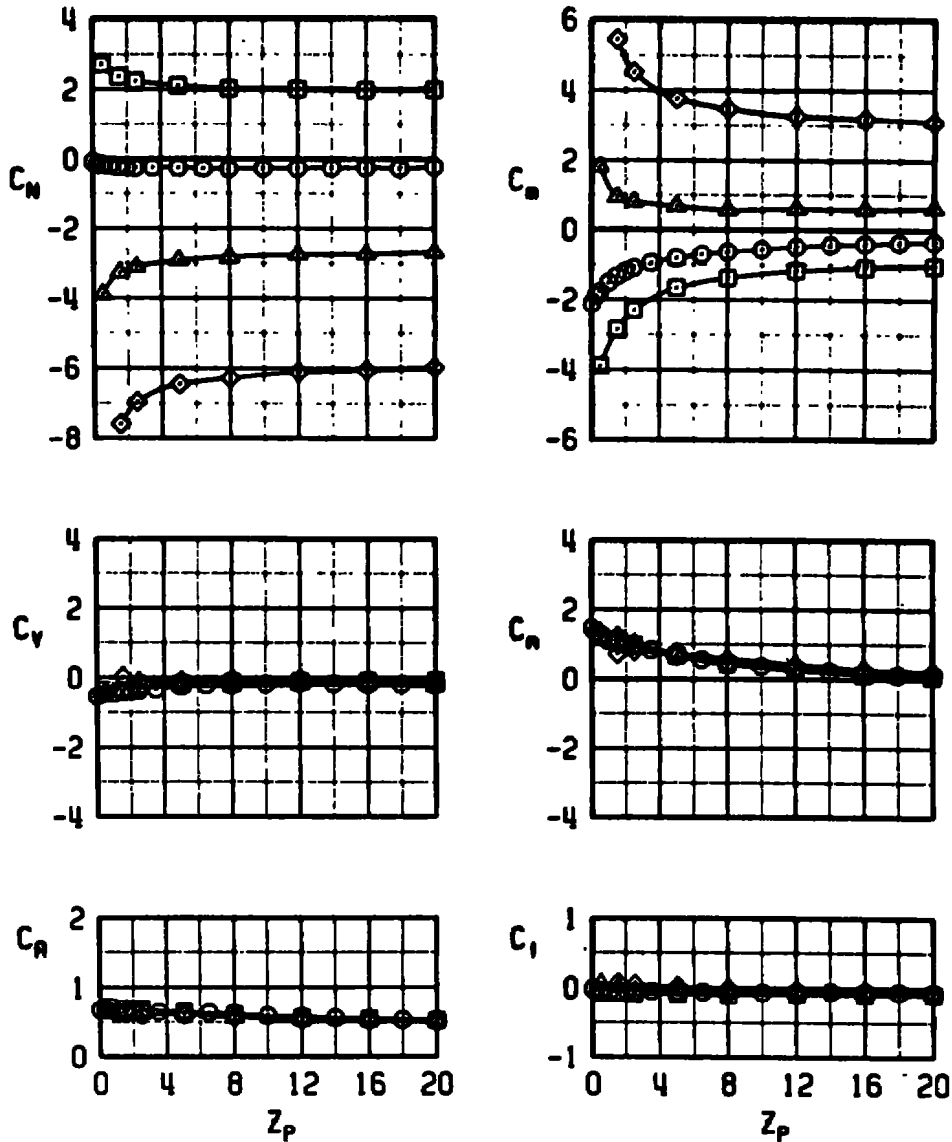
b.  $M_\infty = 0.95$   
Figure 15. Continued.

SYM	$M_\infty$	STORE	$\bullet$
○	1.20	GBU-15 CMW	0
□	1.20	GBU-15 CMW	5
△	1.20	GBU-15 CMW	-5



c.  $M_\infty = 1.2$   
 Figure 15. Concluded.

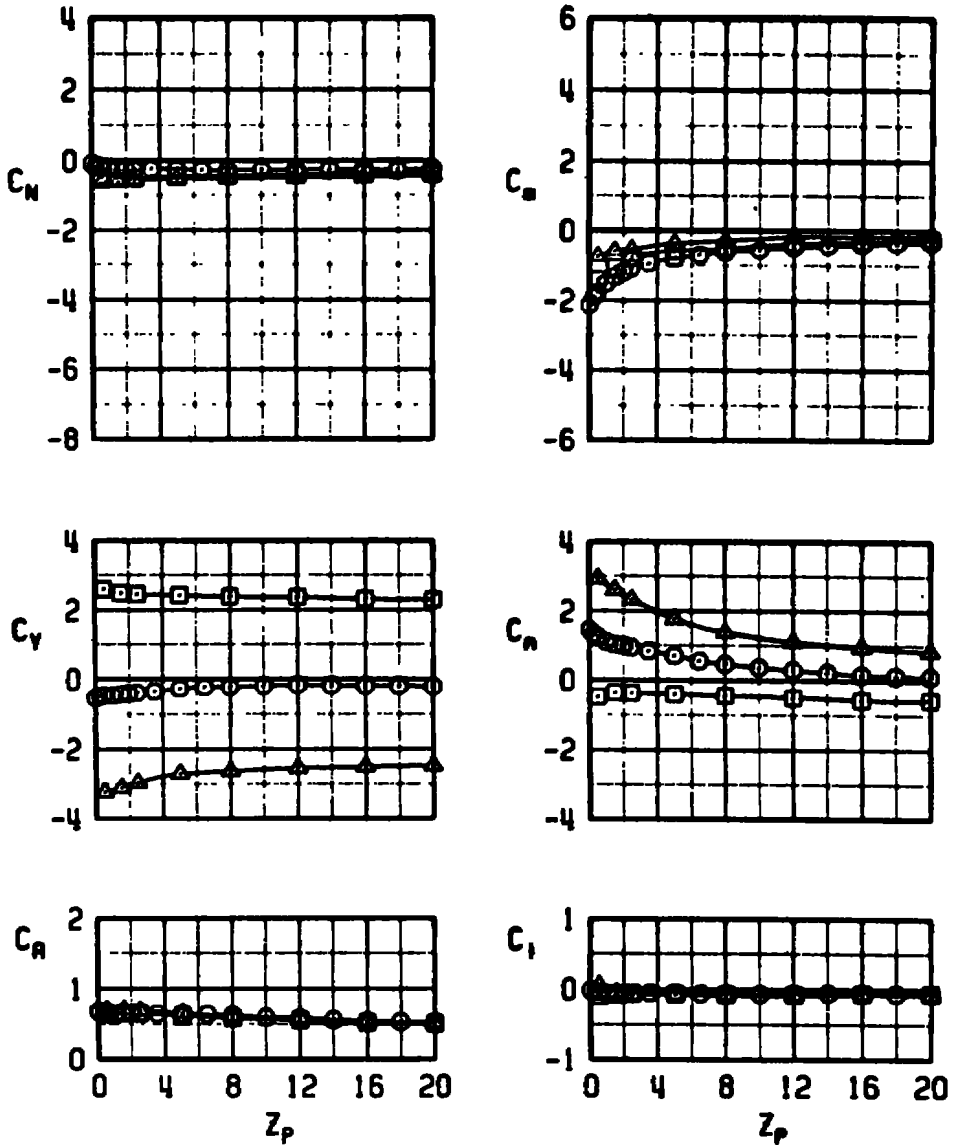
SYM	$M_\infty$	$\alpha$	STORE	$\Delta\theta$
⊙	0.95	0	GBU-15 CWW	0
⊠	0.95	0	GBU-15 CWW	5
⊡	0.95	0	GBU-15 CWW	-5
◇	0.95	0	GBU-15 CWW	-10



a. Effect of pitch angle

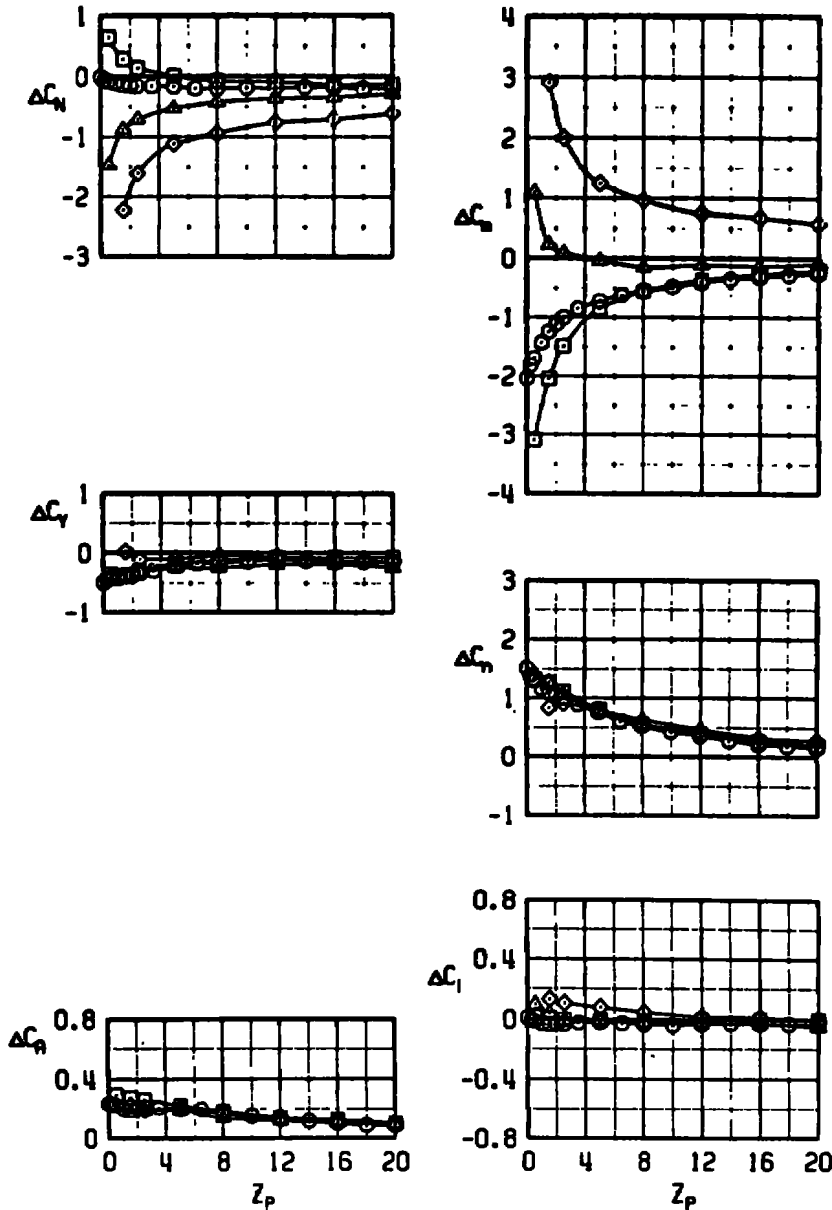
Figure 16. Aerodynamic characteristics of the GBU-15 CWW at various orientations relative to the carriage position.

SYM	M <sub>∞</sub>	α	STORE	Δφ
⊙	0.95	0	GBU-15 CMW	0
□	0.95	0	GBU-15 CMW	5
▲	0.95	GBU-15 CMW	-5	



b. Effect of yaw angle  
Figure 16. Concluded.

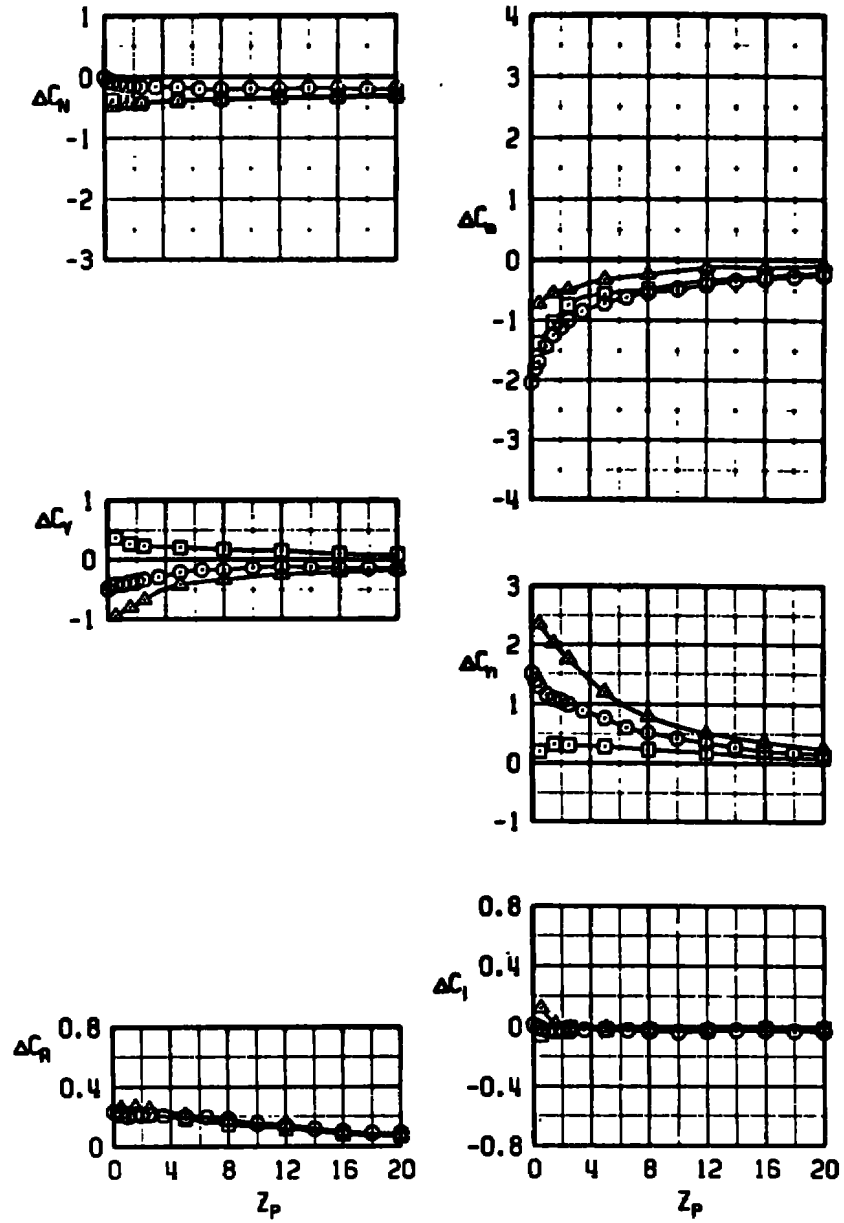
SYM	$M_\infty$	$\alpha$	STORE	$\Delta\theta$
⊙	0.95	0	GBU-15 CWH	0
⊠	0.95	0	GBU-15 CWH	5
△	0.95	0	GBU-15 CWH	-5
◇	0.95	0	GBU-15 CWH	-10



a. Effect of pitch angle

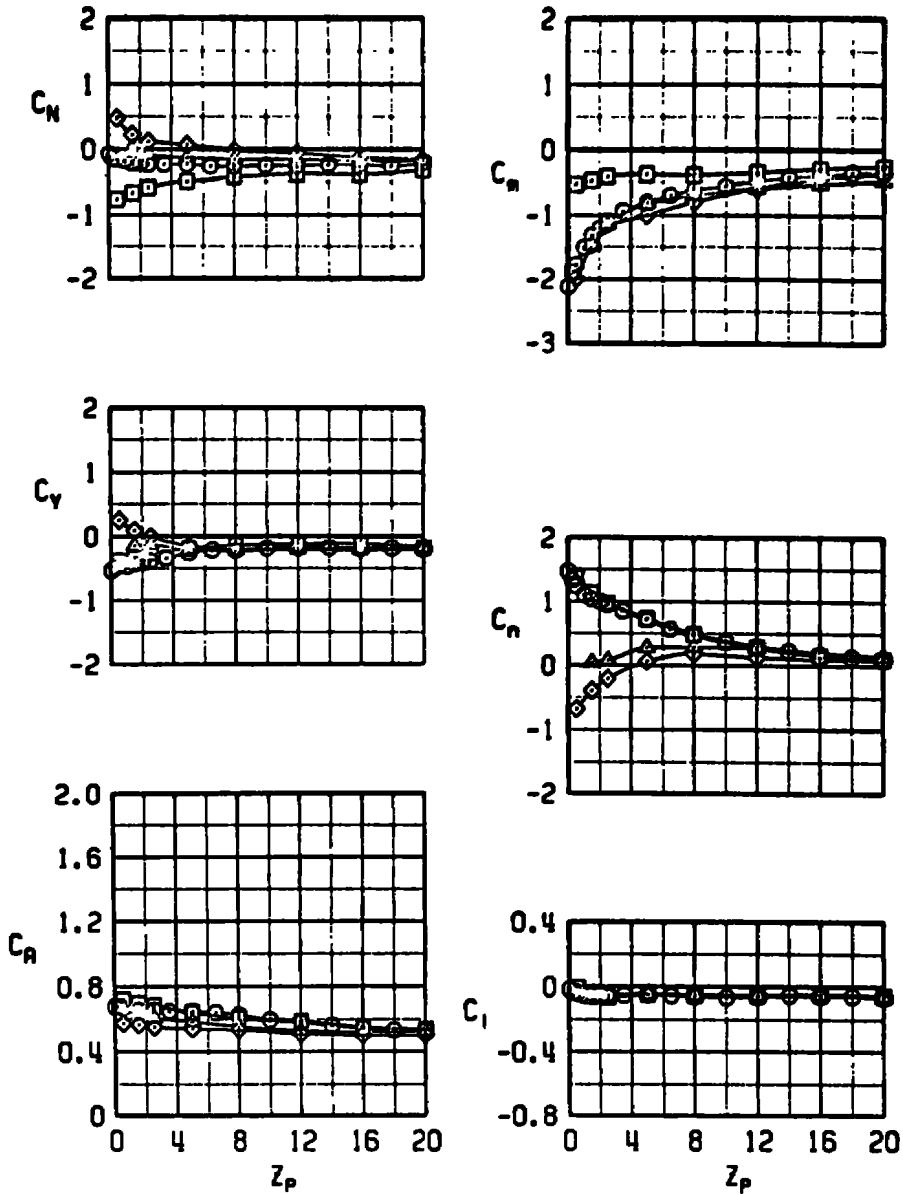
Figure 17. Delta-coefficient data for the GBU-15 CWH at various orientations relative to the carriage position.

SYM	M <sub>∞</sub>	α	STORE	Δθ
○	0.95	0	GBU-15 CMW	0
□	0.95	0	GBU-15 CMW	5
△	0.95	0	GBU-15 CMW	-5



b. Effect of yaw angle  
Figure 17. Concluded.

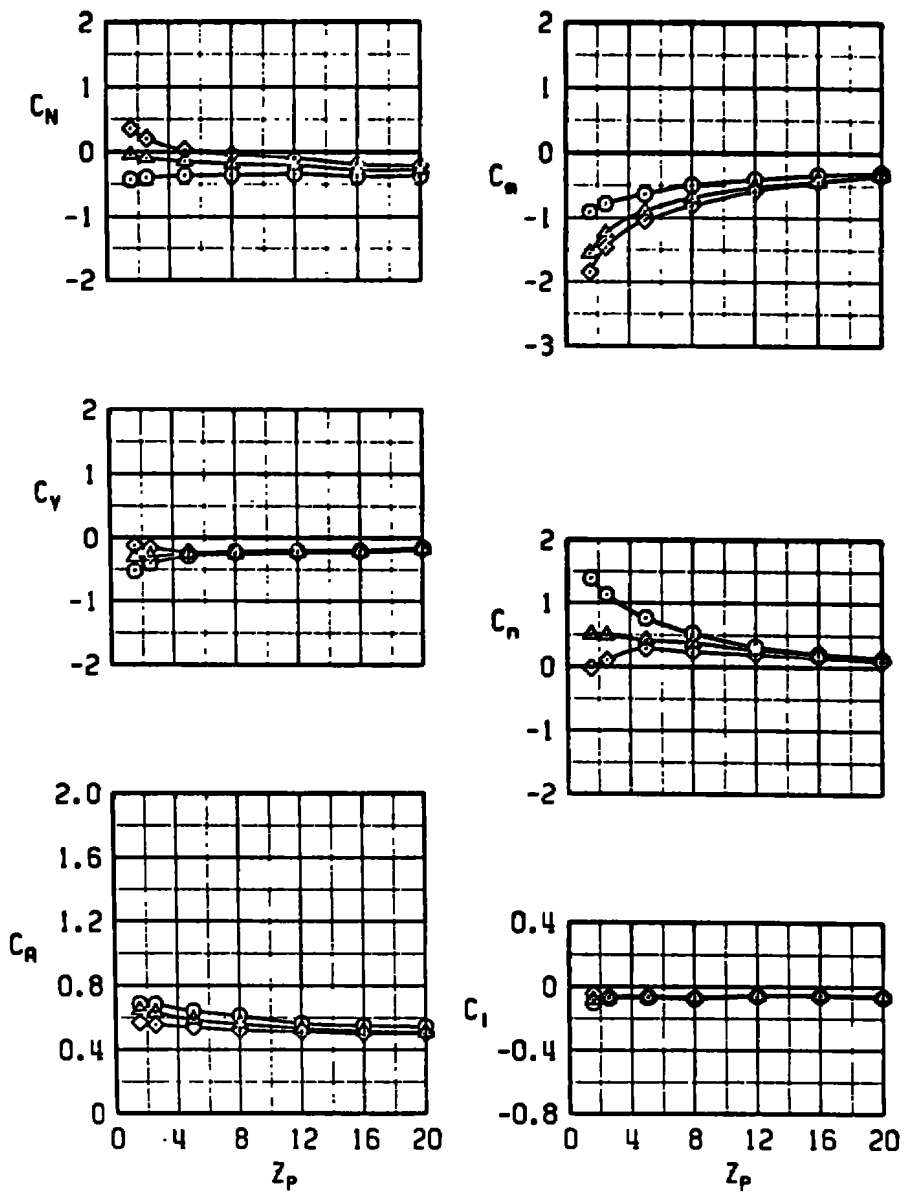
SYM	$M_\infty$	$\alpha$	STORE	$Y_P$	$X_P$
□	0.95	0	GBU-15 CW	0	2
○	0.95	0	GBU-15 CW	0	0
△	0.95	0	GBU-15 CW	0	-2
◇	0.95	0	GBU-15 CW	0	-4



a.  $Y_P = 0$

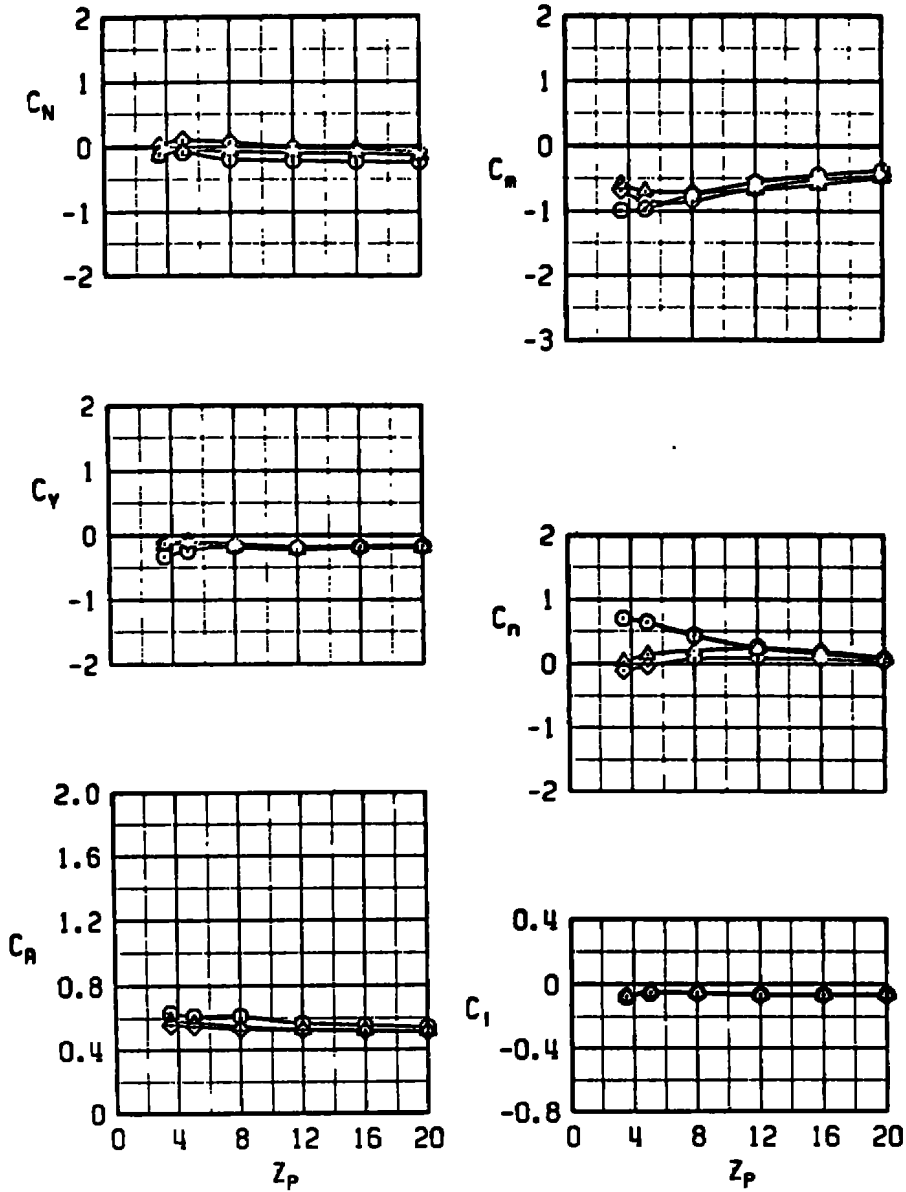
Figure 18. Aerodynamic characteristics showing the effects of varying longitudinal position at constant lateral positions.

SYM	$M_\infty$	$\alpha$	STORE	$Y_p$	$X_p$
○	0.95	0	GBU-15 CWW	2	0
△	0.95	0	GBU-15 CWW	2	-2
◇	0.95	0	GBU-15 CWW	2	-4



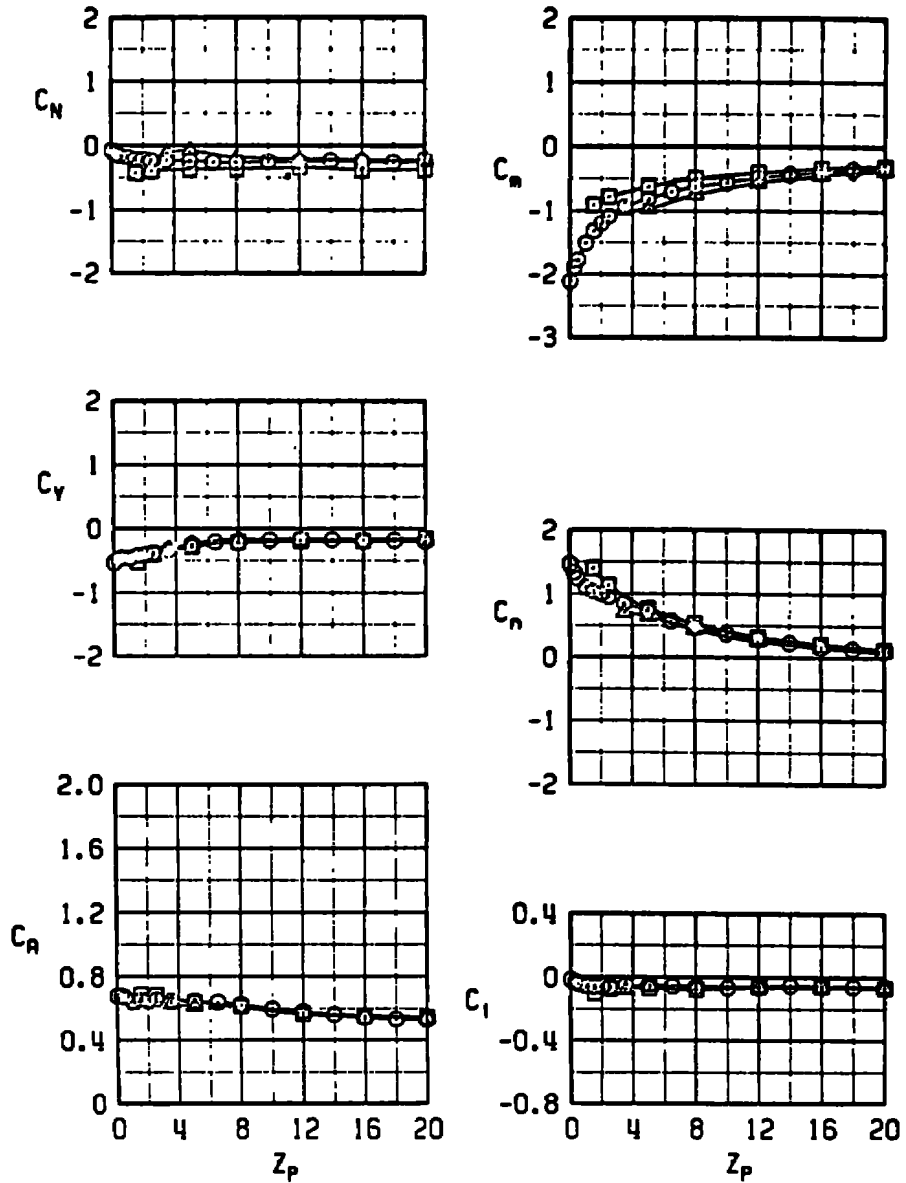
b.  $Y_p = 2$   
Figure 18. Continued.

SYM	$M_\infty$	$\alpha$	STORE	$Y_P$	$X_P$
○	0.95	0	GBU-15 CWH	-2	0
△	0.95	0	GBU-15 CWH	-2	-2
◇	0.95	0	GBU-15 CWH	-2	-4



c.  $Y_P = -2$   
 Figure 18. Concluded.

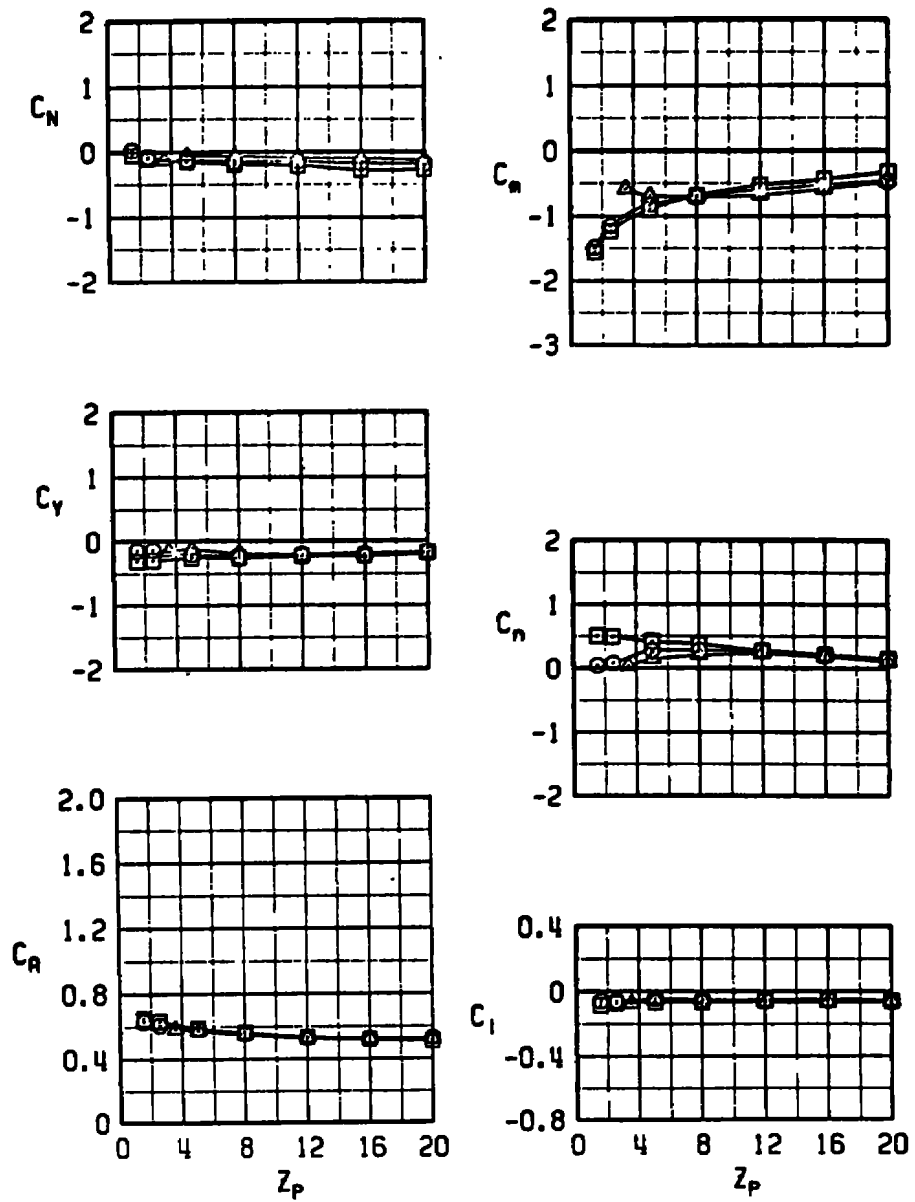
SYM	$M_\infty$	$\alpha$	STORE	$X_p$	$Y_p$
□	0.95	0	GBU-15 CW	0	2
○	0.95	0	GBU-15 CW	0	0
△	0.95	0	GBU-15 CW	0	-2



a.  $X_p = 0$

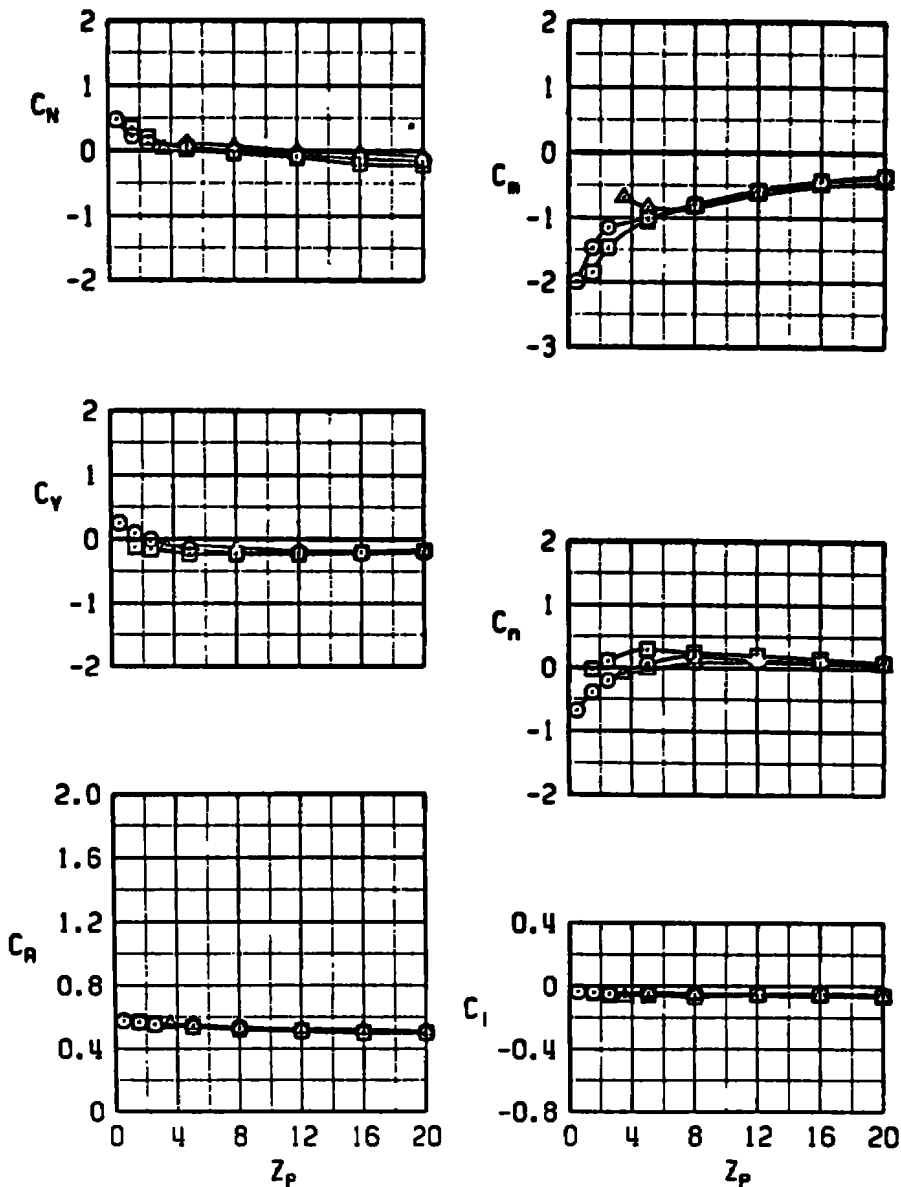
Figure 19. Aerodynamic characteristics showing the effects of varying lateral position at constant longitudinal positions.

SYM	$M_\infty$	$\alpha$	STORE	$X_P$	$Y_P$
□	0.95	0	GBU-15 CW	-2	2
○	0.95	0	GBU-15 CW	-2	0
△	0.95	0	GBU-15 CW	-2	-2



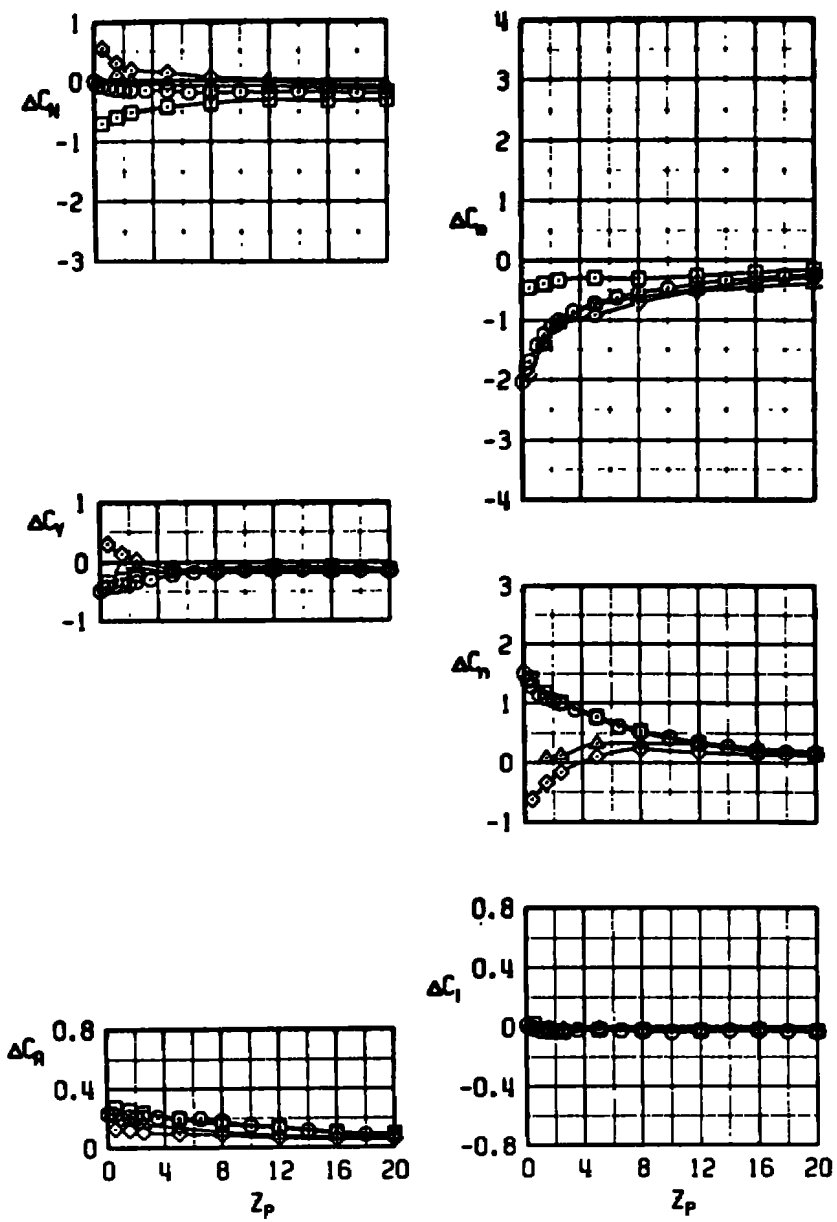
b.  $X_p = -2$   
 Figure 19. Continued.

SYM	$M_\infty$	$\alpha$	STORE	$X_p$	$Y_p$
□	0.95	0	GBU-15 CW	-4	2
○	0.95	0	GBU-15 CW	-4	0
△	0.95	0	GBU-15 CW	-4	-2



c.  $X_p = -4$   
 Figure 19. Concluded.

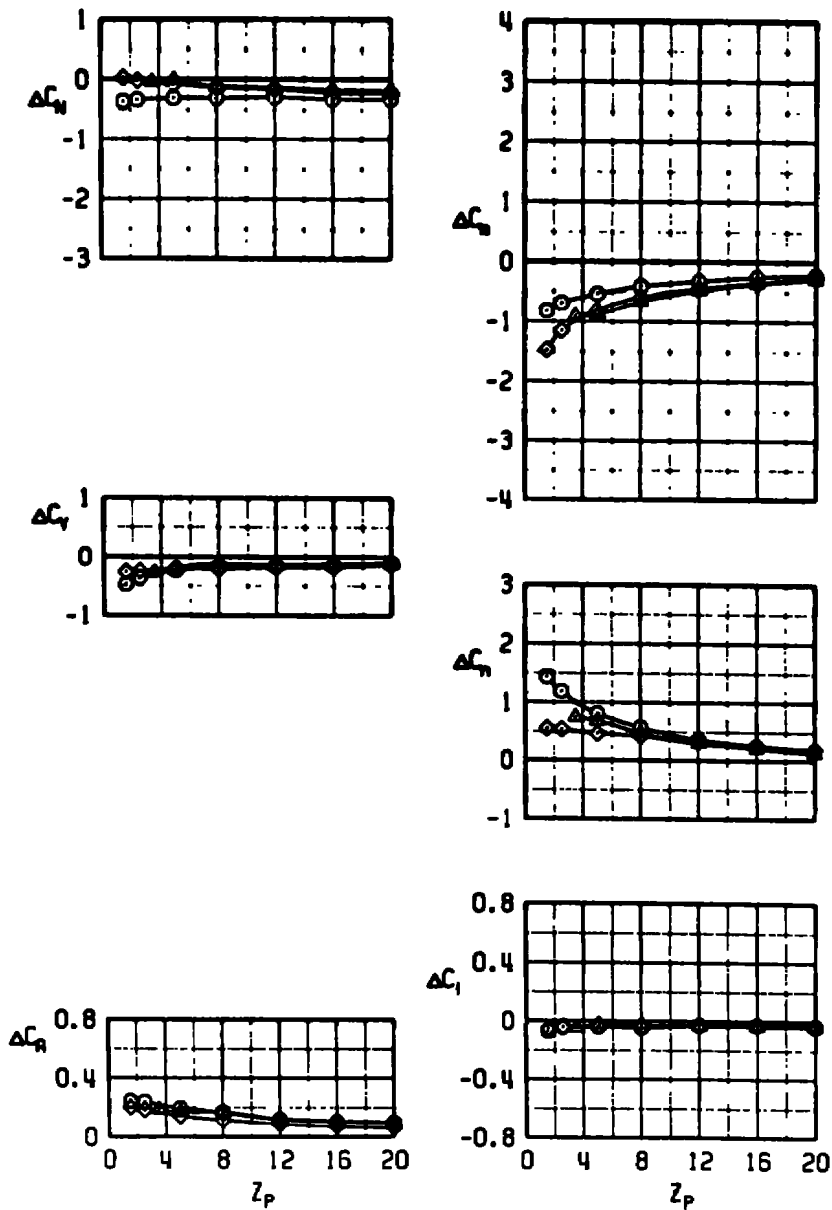
	$N_c$	$\alpha$	STORE	$Y_p$	$X_p$
□	0.95	0	GBU-15 CW	0	2
○	0.95	0	GBU-15 CW	0	0
▲	0.95	0	GBU-15 CW	0	-2
◇	0.95	0	GBU-15 CW	0	-4



a.  $Y_p = 0$

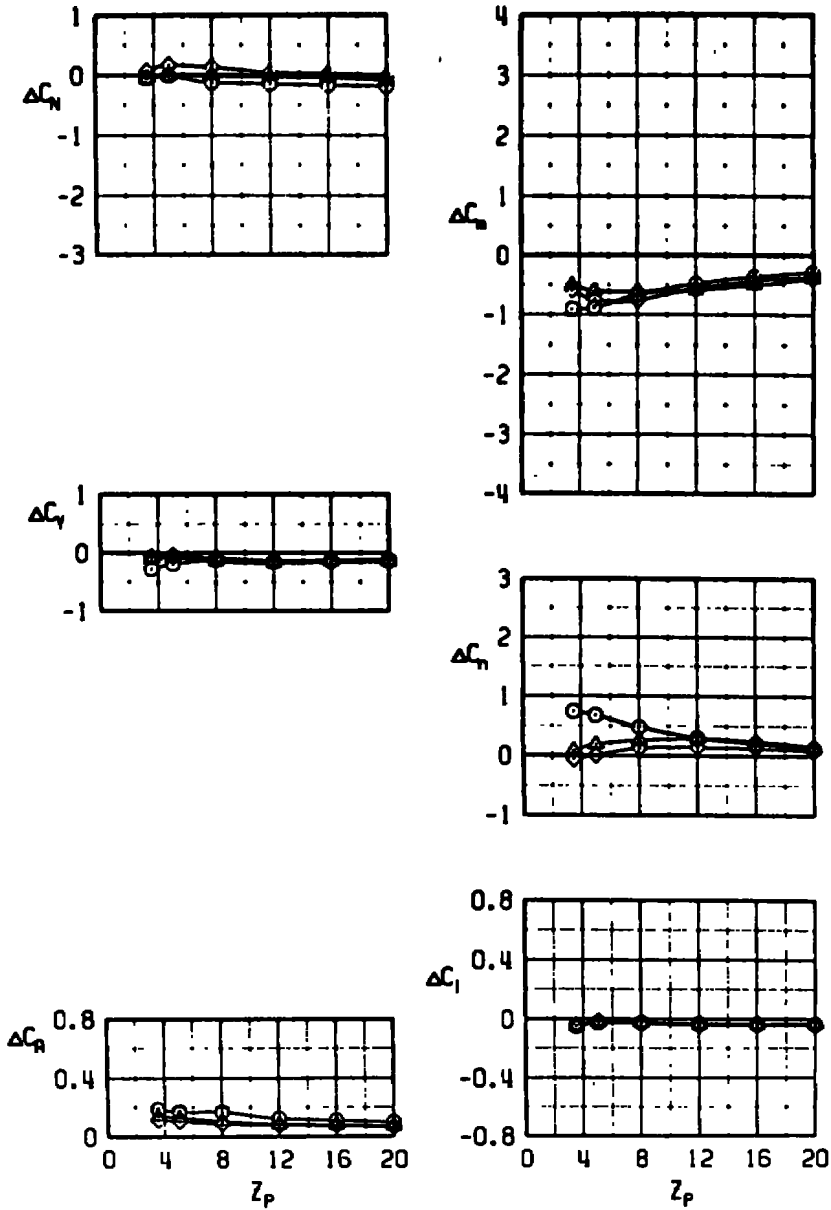
Figure 20. Delta-coefficient data for varying longitudinal and constant lateral positions.

	$M_\infty$	$\alpha$	STORE	$Y_p$	$X_p$
○	0.95	0	GBU-15 CMW	2	0
▲	0.95	0	GBU-15 CMW	2	-2
◇	0.95	0	GBU-15 CMW	2	-4



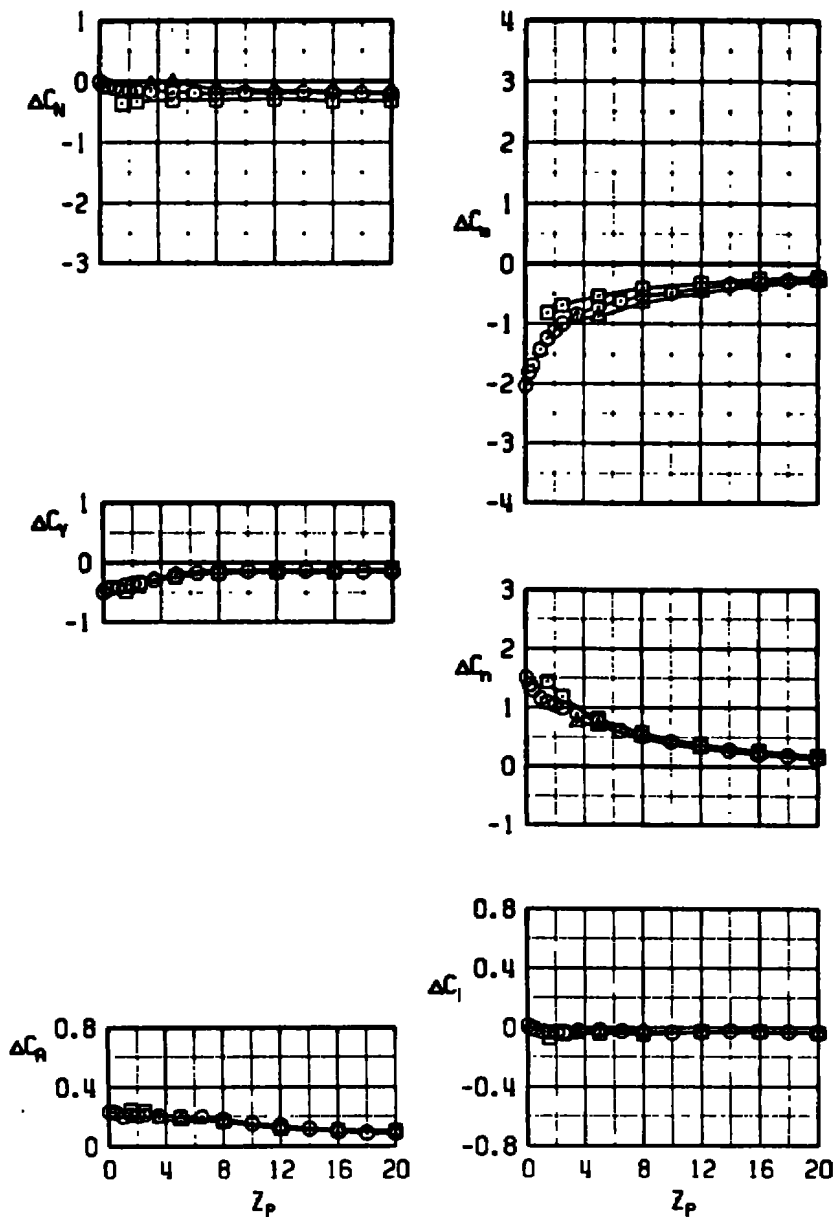
b.  $Y_p = 2$   
Figure 20. Continued.

	$M_\infty$	$\alpha$	STORE	$Y_P$	$X_P$
○	0.95	0	GBU-15 CWM	-2	0
△	0.95	0	GBU-15 CWM	-2	-2
◇	0.95	0	GBU-15 CWM	-2	-4



c.  $Y_P = -2$   
 Figure 20. Concluded.

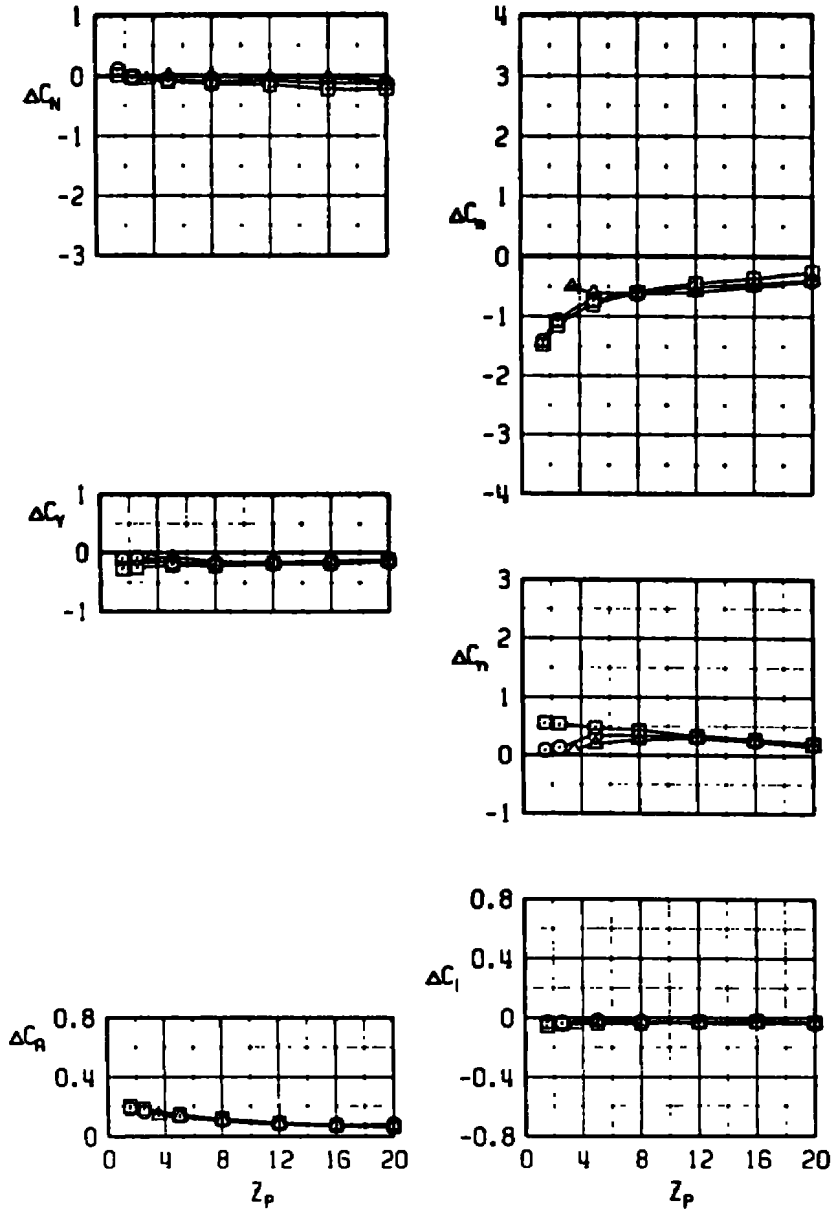
	$M_\infty$	$\alpha$	STORE	$X_p$	$Y_p$
□	0.95	0	GBU-15 CW	0	2
○	0.95	0	GBU-15 CW	0	0
△	0.95	0	GBU-15 CW	0	-2



a.  $X_p = 0$

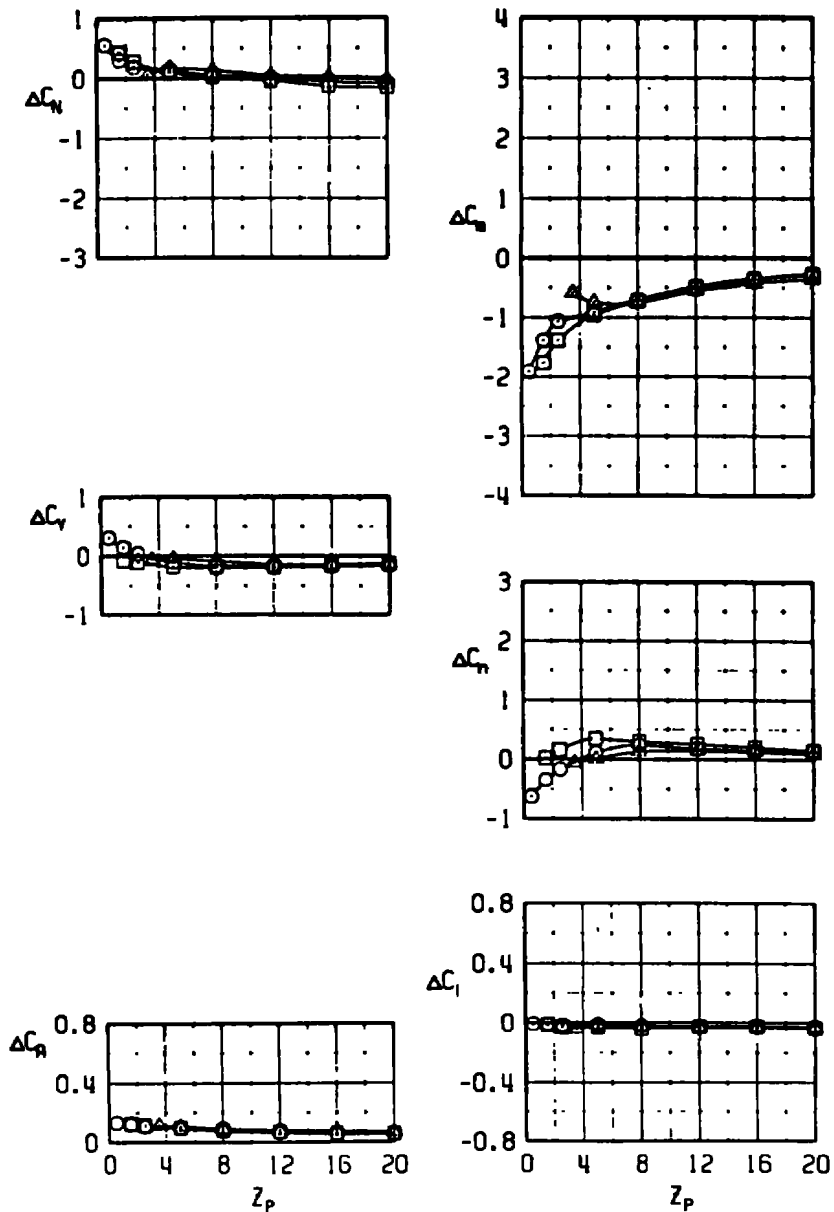
Figure 21. Delta-coefficient data for varying lateral and constant longitudinal positions.

	$M_\infty$	$\alpha$	STORE	$X_p$	$Y_p$
□	0.95	0	GBU-15 CWH	-2	2
○	0.95	0	GBU-15 CWH	-2	0
△	0.95	0	GBU-15 CWH	-2	-2



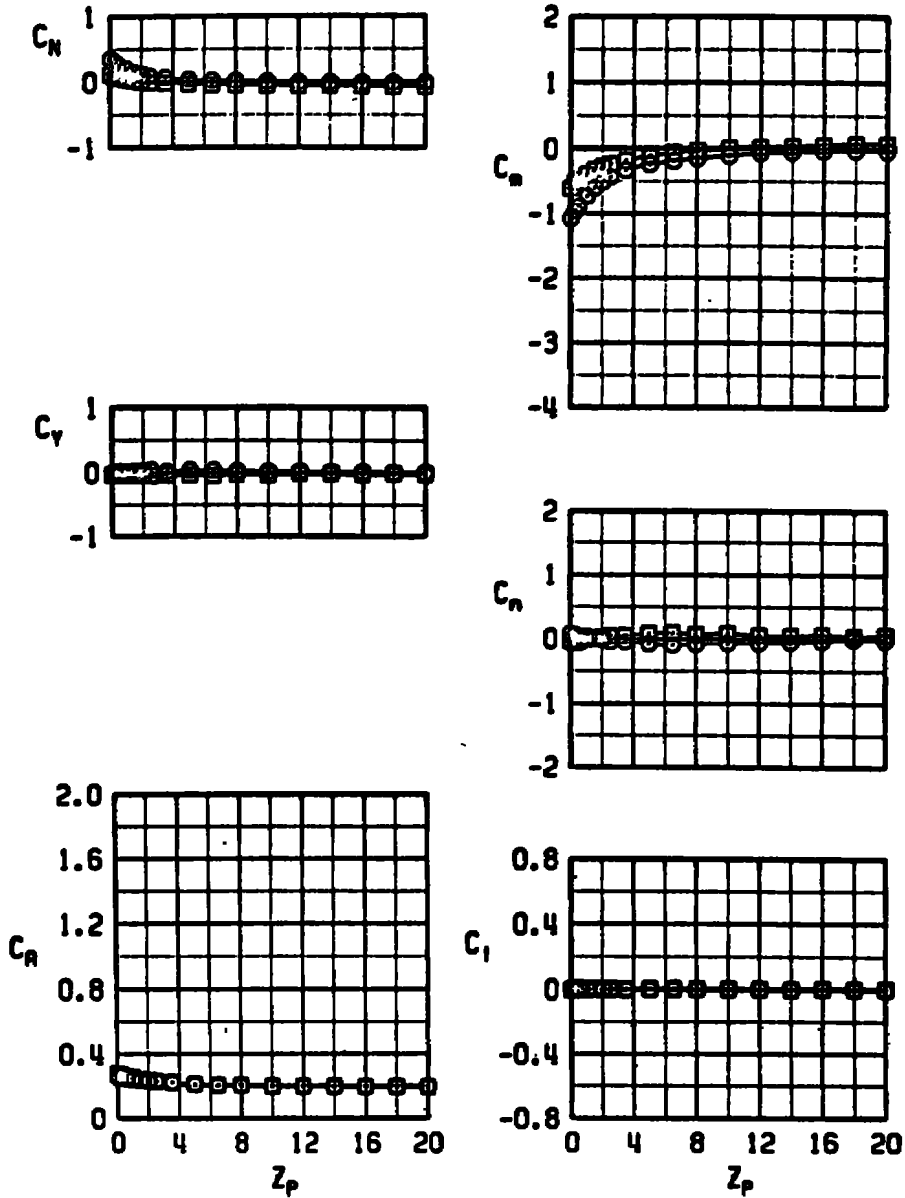
b.  $X_p = -2$   
 Figure 21. Continued.

	$M_\infty$	$\alpha$	STORE	$X_p$	$Y_p$
□	0.95	0	GBU-15 CWH	-4	2
○	0.95	0	GBU-15 CWH	-4	0
△	0.95	0	GBU-15 CWH	-4	-2



c.  $X_p = -4$   
 Figure 21. Concluded.

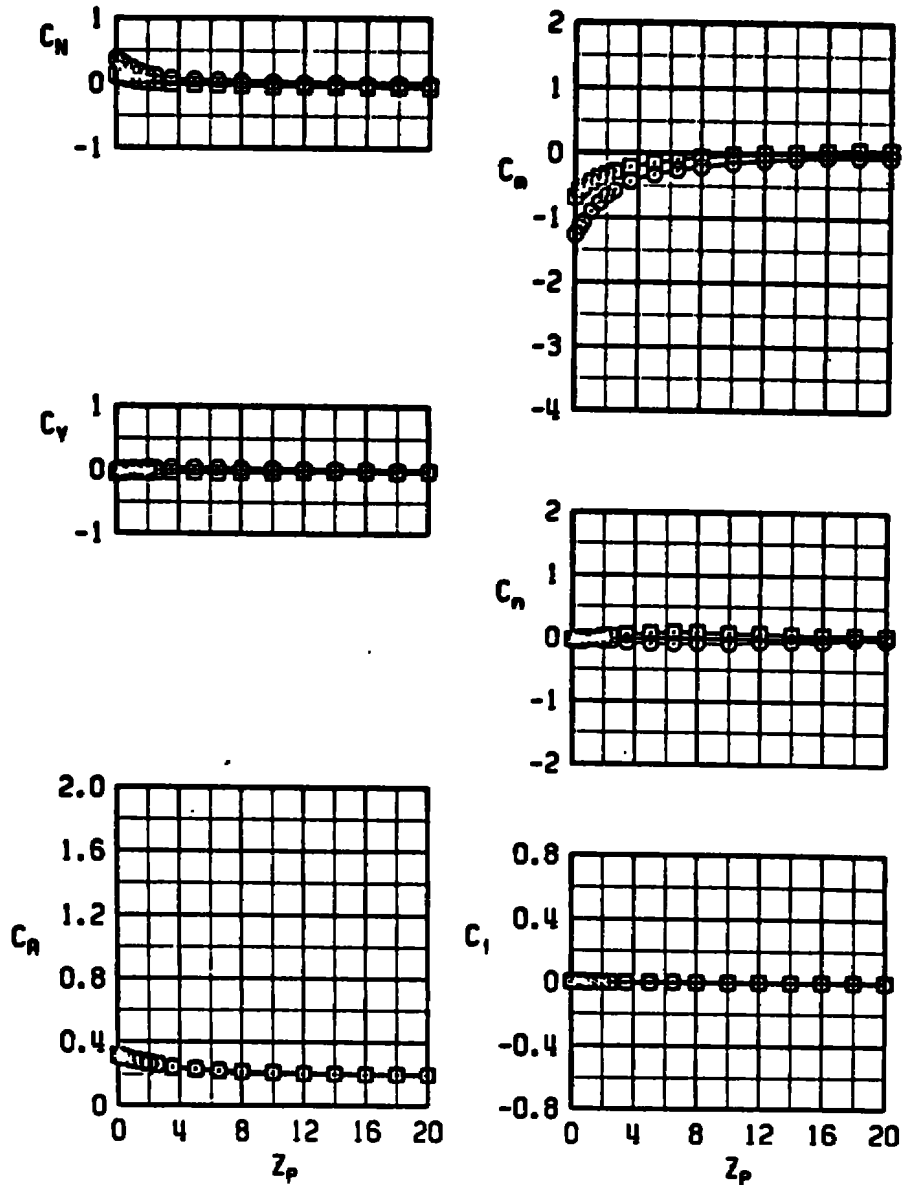
	$M_\infty$	$\alpha$	STORE	CONFIG
□	0.80	0	MK-84 LDGP	9
○	0.80	0	MK-84 LDGP	10



a.  $M_\infty = 0.8$

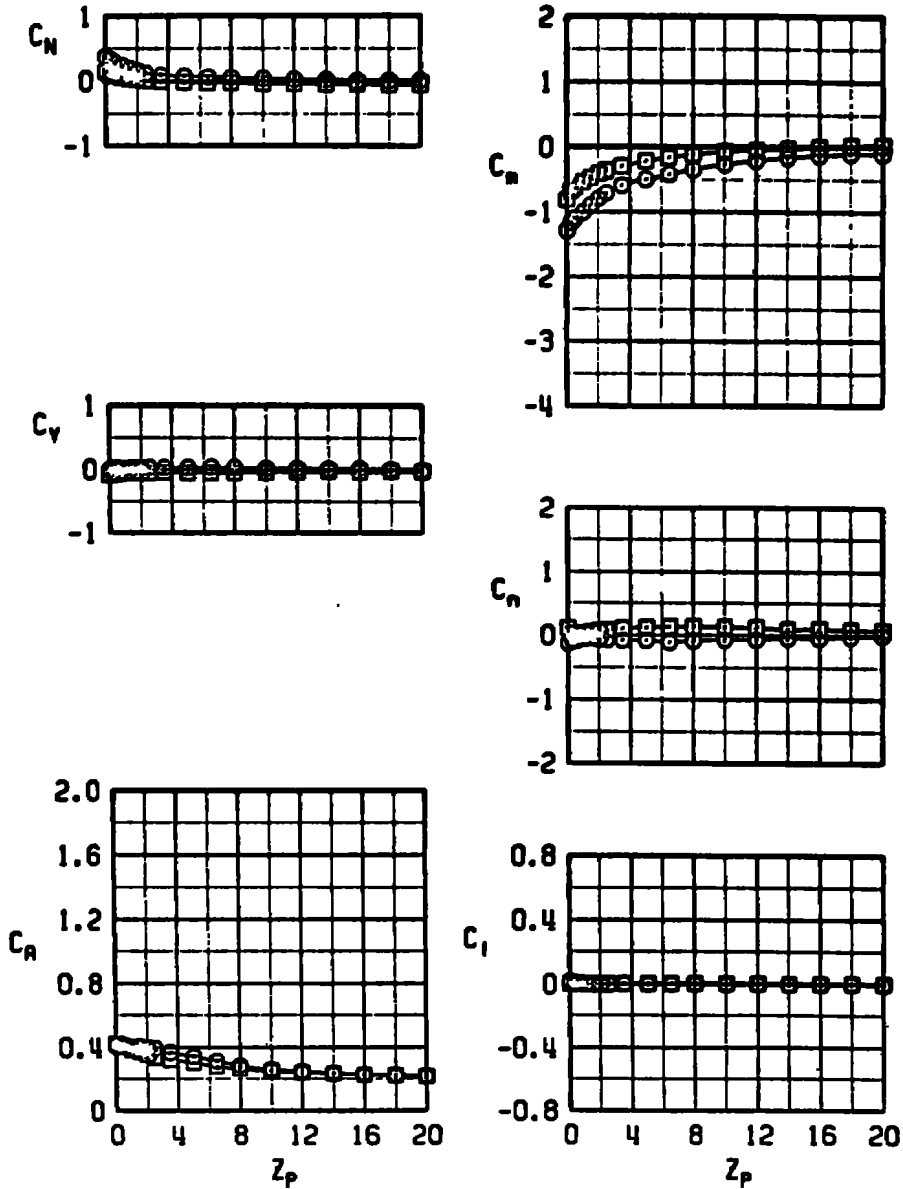
Figure 22. Effects of the AIM-9 missiles and launchers on the aerodynamic characteristics of the MK-84 LDGP.

	$M_\infty$	$\alpha$	STORE	CONFIG
□	0.90	0	MK-84 LOGP	9
○	0.90	0	MK-84 LOGP	10



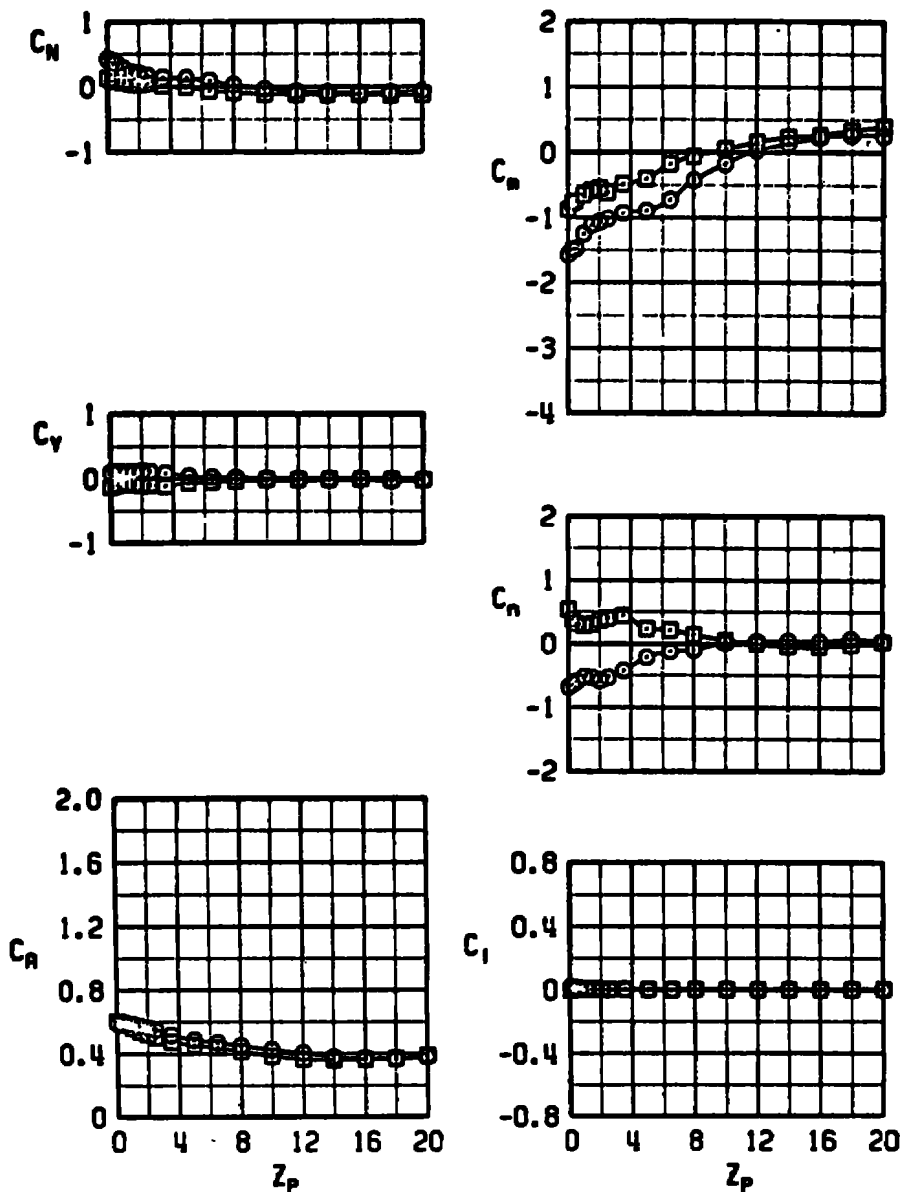
b.  $M_\infty = 0.9$   
 Figure 22. Continued.

	$M_\infty$	$\alpha$	STORE	CONFIG
□	0.95	0	MK-84 LDGP	9
○	0.95	MK-84 LDGP	10	



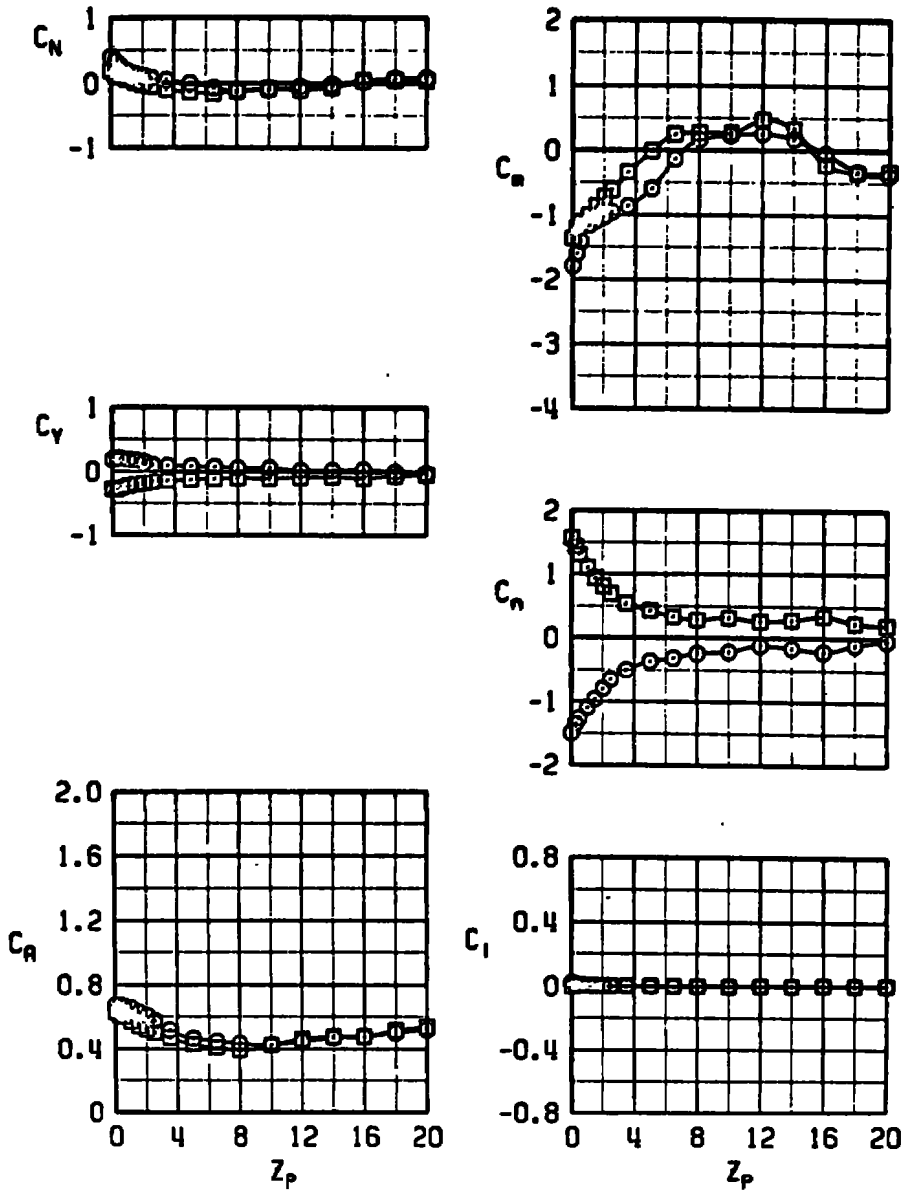
c.  $M_\infty = 0.95$   
 Figure 22. Continued.

	$M_\infty$	$\alpha$	STORE	CONFIG
□	1.05	0	MK-84 LDGP	9
○	1.05	0	MK-84 LDGP	10



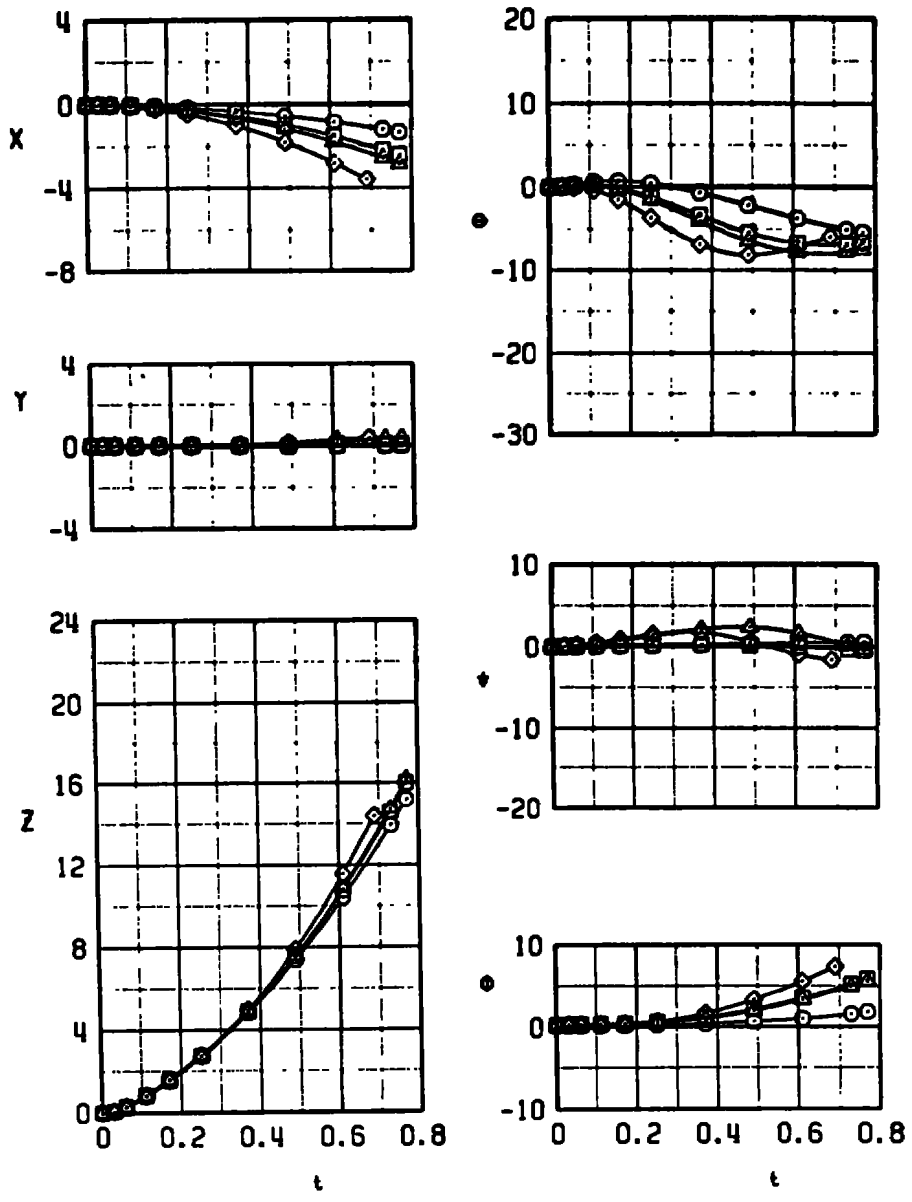
d.  $M_\infty = 1.05$   
 Figure 22. Continued.

	$M_\infty$	$\alpha$	STORE	CONFIG
□	1.20	0	MK-84 LDGP	9
○	1.20	0	MK-84 LDGP	10



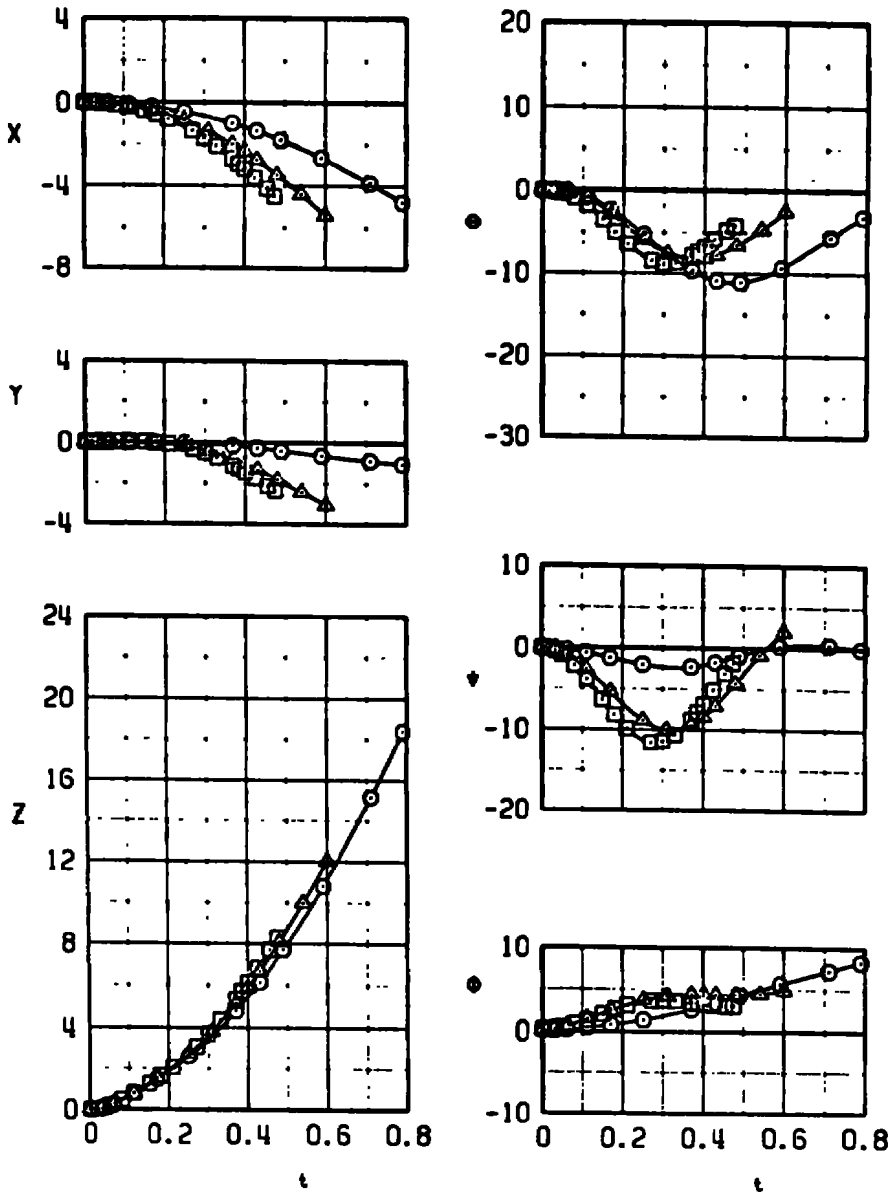
e.  $M_\infty = 1.2$   
 Figure 22. Concluded.

	$M_\infty$	$\alpha$	STORE	CONFIG	H
⊙	0.67	0.5	GBU-10	7	5.5K
⊠	0.83	0.5	GBU-10	7	5.5K
△	0.95	0.5	GBU-10	7	15.8K
◇	0.95	0.5	GBU-10	7	5.0K



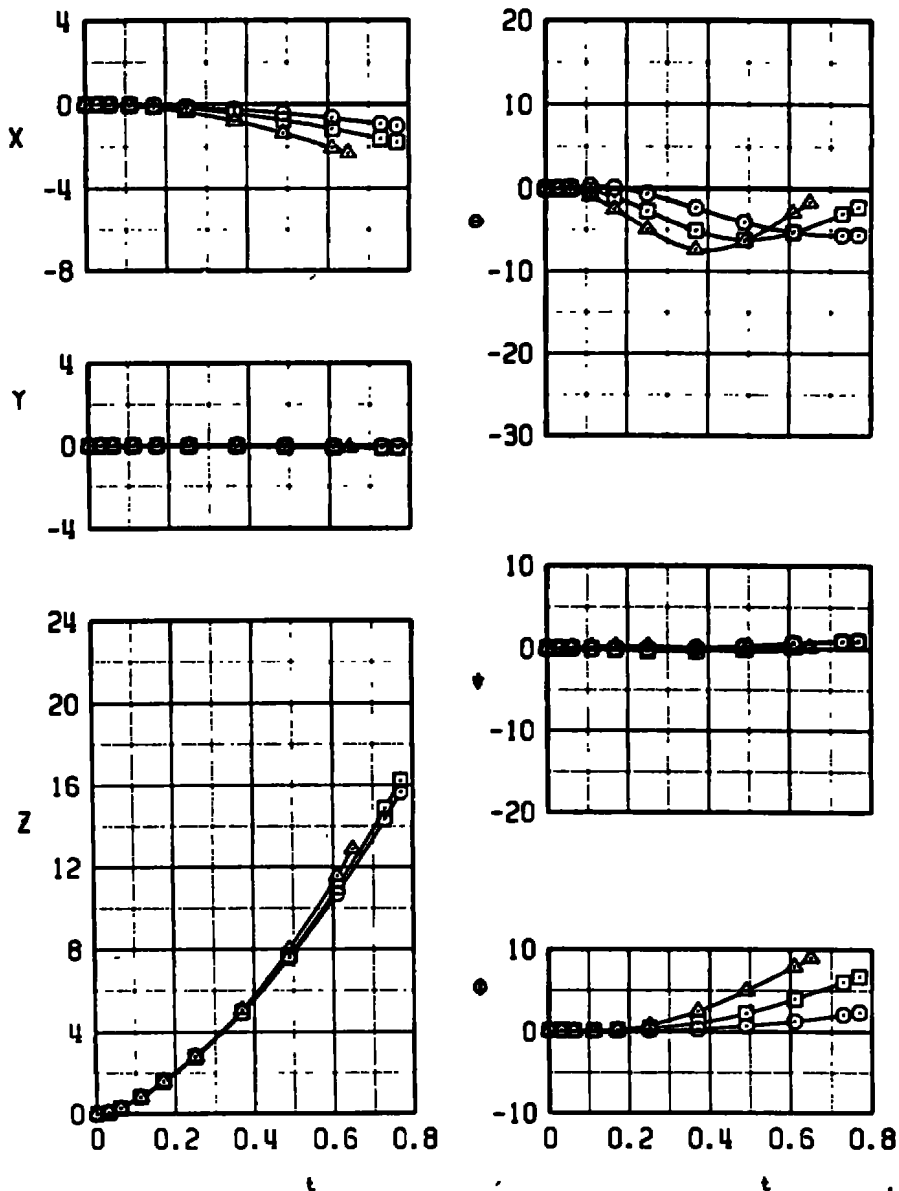
a.  $M_\infty = 0.67, 0.83, \text{ and } 0.95$   
**Figure 23. Separation characteristics of the GBU-10 from the F-15 aircraft.**

	$M_\infty$	$\alpha$	STORE	CONFIG	H
○	0.95	0.5	GBU-10	8	5.0K
□	1.21	0.5	GBU-10	8	9.1K
△	1.30	0.5	GBU-10	8	18.0K



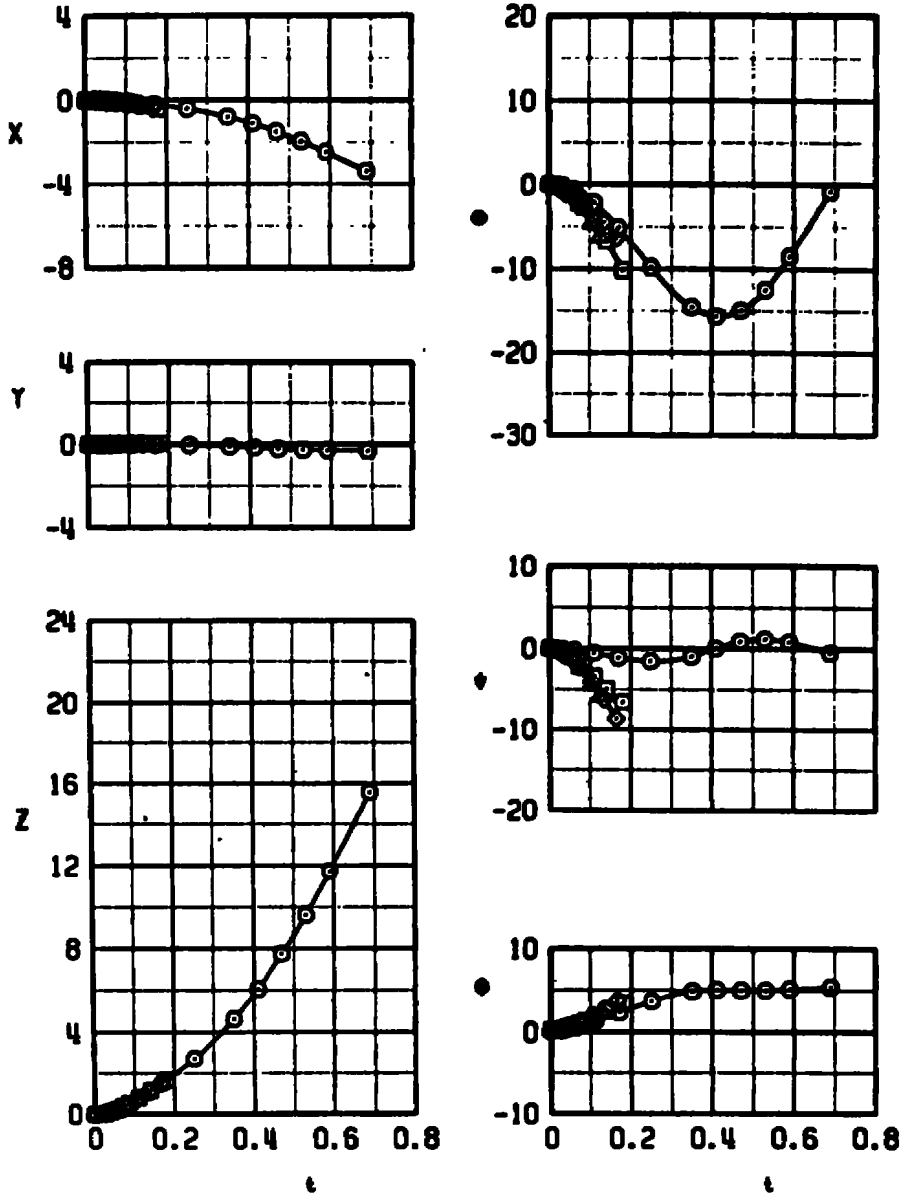
b.  $M_\infty = 0.95, 1.21, \text{ and } 1.30$   
 Figure 23. Concluded.

	$M_\infty$	$\alpha$	STORE	CONFIG	H
○	0.66	0.5	MK-84 LDGP	9	5.3K
□	0.83	0.5	MK-84 LDGP	9	5.3K
△	0.95	0.5	MK-84 LDGP	9	5.9K



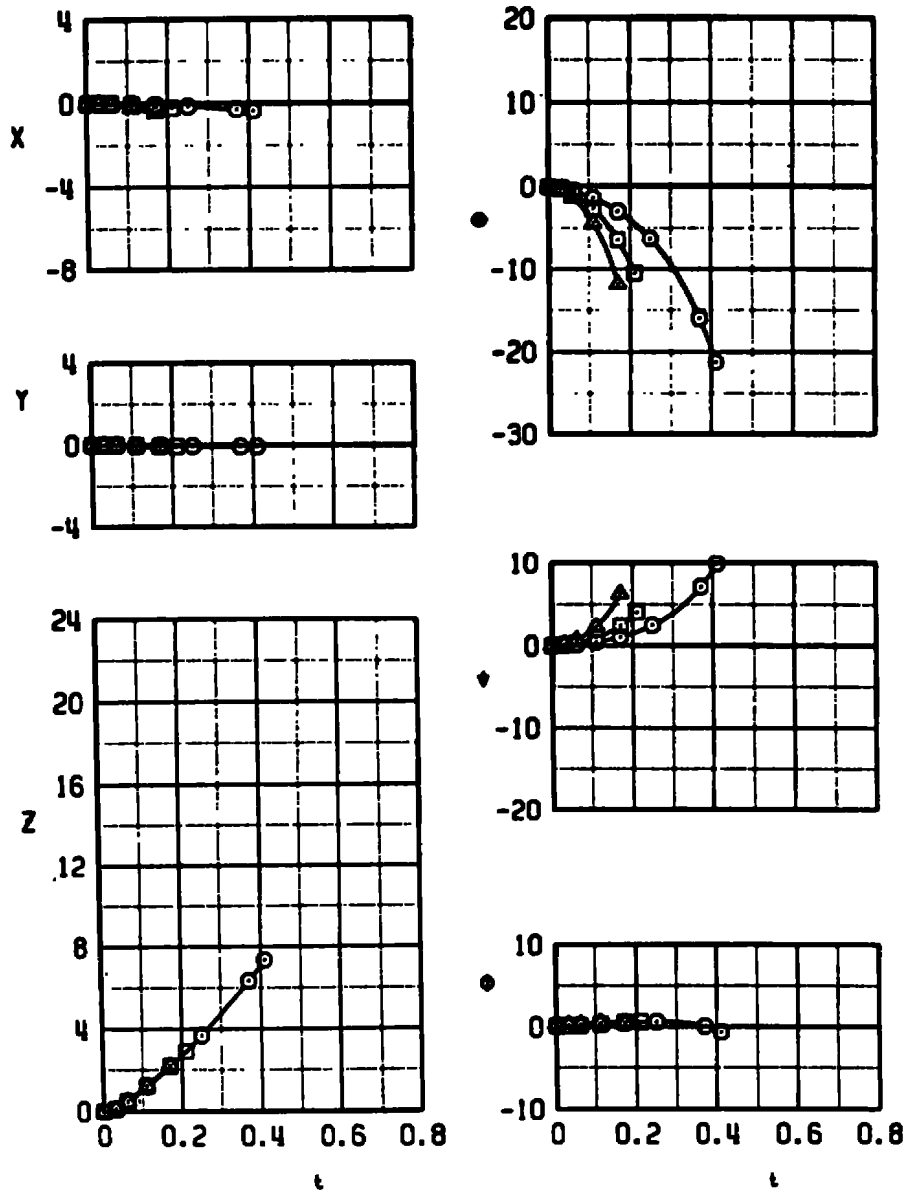
a.  $M_\infty = 0.66, 0.83, \text{ and } 0.95$   
**Figure 24. Separation characteristics of the MK-84 LDGP from the F-15 aircraft.**

	$M_\infty$	$\alpha$	STORE	CONFIG	H
○	0.95	0.5	MK-84 LDGP	IO	5.9K
□	1.10	0.5	MK-84 LDGP	IO	9.0K
△	1.19	0.5	MK-84 LDGP	IO	10.0K
◇	1.30	0.5	MK-84 LDGP	IO	18.0K



b.  $M_\infty = 0.95, 1.1, 1.19, \text{ and } 1.3$   
 Figure 24. Concluded.

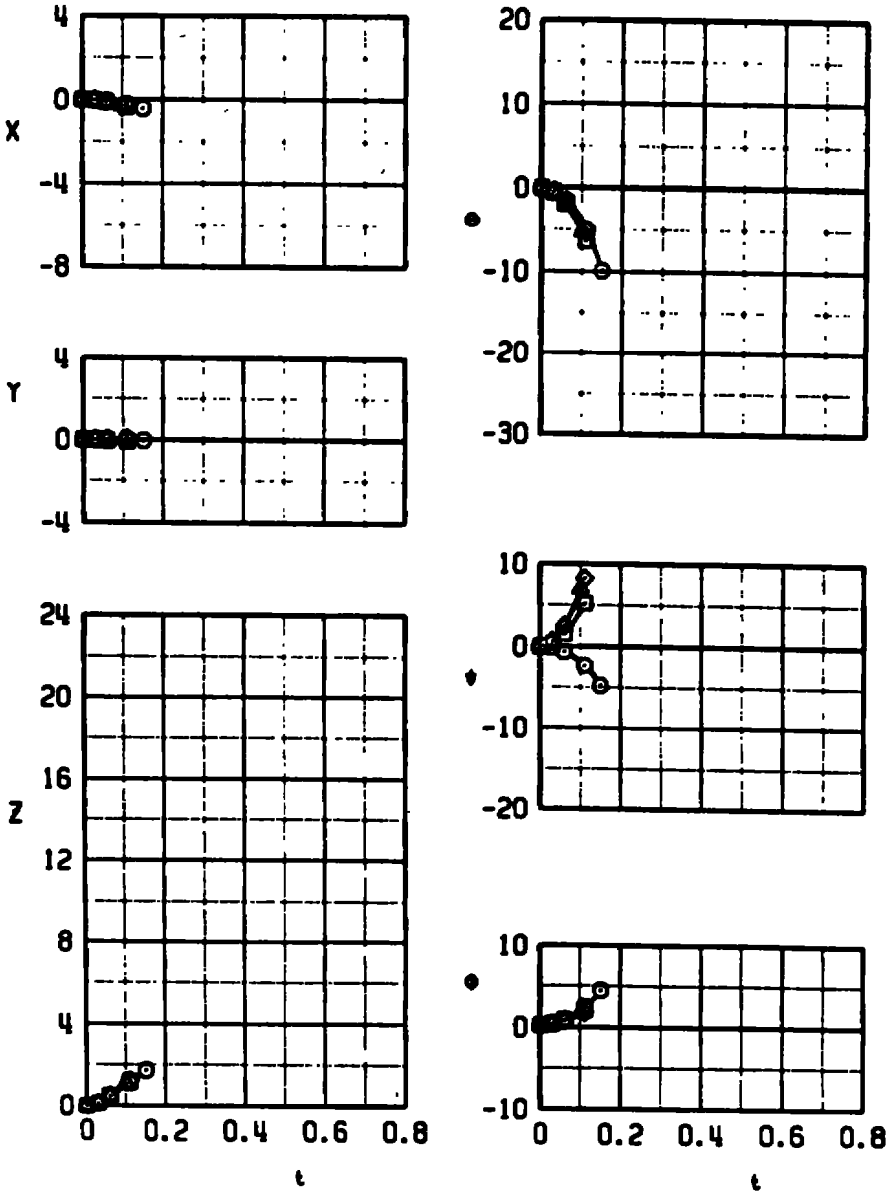
	$M_\infty$	STORE	CONFIG	H
○	0.60	0.5 BLU-27 (U)	13	5.0K
□	0.80	0.5 BLU-27 (U)	13	5.0K
△	0.95	0.5 BLU-27 (U)	13	5.0K



a.  $M_\infty = 0.6, 0.8, \text{ and } 0.95$

Figure 25. Separation characteristics of the BLU-27B/B(U) from the F-15 aircraft.

	$M_\infty$	$\alpha$	STORE	CONFIG	H
○	0.95	0.5	BLU-27 (U)	14	5.0K
□	1.10	0.5	BLU-27 (U)	13	9.0K
△	1.20	0.5	BLU-27 (U)	13	10.0K
◇	1.30	0.5	BLU-27 (U)	13	18.0K



b.  $M_\infty = 0.95, 1.1, 1.2, \text{ and } 1.3$   
 Figure 25. Concluded.

**Table 1. Test Summary – Aerodynamic Loads**  
**a. Store Positions and Schedules**

<u>X</u>	<u>Y</u>	<u>Z</u>	<u><math>\Delta\psi</math></u>	<u><math>\Delta\theta</math></u>	<u><math>\Delta\phi</math></u>	<u>Schedule A</u>	<u>Schedule B</u>	<u>Schedule C</u>
0	0	0-20	0	0	0	*	*	*
		0.5-20	0	$\pm 5$	0	*		
		1.5-20	0	-10	0	*		
		2.5-20	0	-20	0	*		
		0.5-20	$\pm 5$	0	0	*		
		0.5-20	0	0	$\pm 10$	*		
		0.5-20	-3.5	-3.5	0	*		
		1.5-20	-7.1	-7.1	0	*		
		2.5-20	-14.2	-14.2	0	*		
$\pm 2$	0	0.5-20	0	0	0	*	*	
0	$\pm 2$	1.5-20	0	0	0	*	*	
-2	$\pm 2$	1.5-20	0	0	0	*	*	
-4	0	0.5-20	0	0	0	*	*	
-4	$\pm 2$	1.5-20	0	0	0	*	*	
—	—	—	0	-30→12	0	Free Stream		
—	—	—	↓	↓	$\pm 10$	↓		
—	—	—			-22.5			
—	—	—	↓		-45			
—	—	—	$\pm 5$	↓	0			

Table 1. Continued  
b. Grid Survey-Number Summary

Store	Config.	Schedule	$\alpha$	$M_\infty$					
				0.6	0.8	0.9	0.95	1.05	1.20
GBU-15 CWW	1	A	0	---	171	175	179	183	187
		A	2	167	---	---	---	---	---
		B	2	---	173	177	181	185	189
		C	4	168	174	178	182	186	190
		B	6	169	---	---	---	---	---
		C	10	170	---	---	---	---	---
	0	Free Stream*		161	162	163	164	165	166
GBU-15 PWW	3	A	0	---	195	199	203	207	211
		A	2	191	---	---	---	---	---
		B	2	---	197	201	205	209	213
		C	4	192	198	202	206	210	214
		B	6	193	---	---	---	---	---
		C	10	194	---	---	---	---	---
	4	C	0	---	196	200	204	208	212
	0	Free Stream		155	156	157	158	159	160
GBU-8	5	A	0	---	219	224	223	227	231
		A	2	215	---	---	---	---	---
		B	2	---	221	226	225	229	233
		C	4	216	222	227	226	230	234
		B	6	217	---	---	---	---	---
		C	10	218	---	---	---	---	---
	6	C	0	---	220	225	224	228	232
	0	Free Stream		149	150	151	152	153	154

\*Maximum  $\alpha_s$  Limited by Balance Loads

**Table 1. Concluded  
b. Grid Survey-Number Summary**

Store	Config.	Schedule	$\alpha$	$M_\infty$					
				0.6	0.8	0.9	0.95	1.05	1.20
GBU-10	7	A	0	---	105	109	113	117	121
		A	2	101	---	---	---	---	---
		B	2	---	107	111	115	119	123
			4	102	108	112	116	120	124
			6	103	---	---	---	---	---
			10	104	---	---	---	---	---
	8	C	0	---	106	110	114	118	122
	0	Free Stream		143	144	145	146	147	148
MK-84 LDGP	9	A	0	---	81	85	89	93	97
		A	2	77	---	---	---	---	---
		B	2	---	83	87	91	95	99
			4	78	84	88	92	96	100
			6	79	---	---	---	---	---
			10	80	---	---	---	---	---
	10	C	0	---	82	86	90	94	98
	0	Free Stream		131	132	133	134	135	136
BLU-27 (U)	13	A	0	---	57	61	65	69	73
		A	2	53	---	---	---	---	---
		B	2	---	59	63	67	71	75
			4	54	60	64	68	72	76
			6	55	---	---	---	---	---
			10	56	---	---	---	---	---
	14	C	0	---	58	62	66	70	74
	0	Free Stream		125	126	127	128	129	130

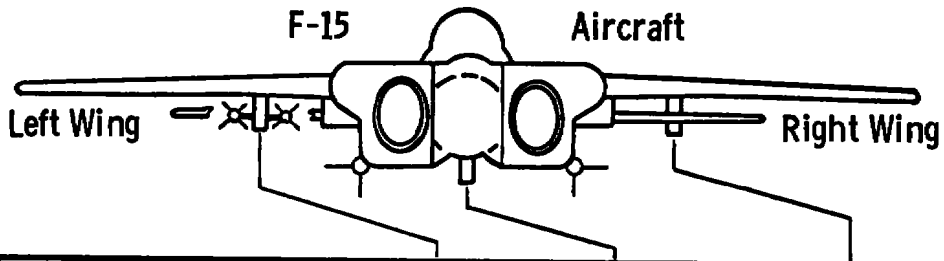
Table 2. Test Summary – Separation Trajectories

Traj	Store	Config	$\alpha$	$M_\infty$	Alt	$F_{Z_1}$	$F_{Z_2}$
1	GBU-10	7	0.5	0.67	5,500	4,000	4,000
2				0.83	5,500		
3				0.95	15,800		
4		↓		↓	5,000		
5		8		↓	5,000		
6		↓		1.21	9,100		
7		↓		1.30	18,000		
8	MK-84 LDGP	9		0.66	5,300		
9		↓		0.83	5,300		
10		↓		0.95	5,900		
11		10		0.95	5,900		
12		↓		1.10	9,000		
13		↓		1.19	10,000		
14		↓		1.30	18,000	↓	↓
15	BLU-27 (U)	13		0.60	5,000	3,200	2,800
16		↓		0.80	↓		
17		↓		0.95	↓		
18		14		0.95	↓		
19		13		1.10	9,000		
20		↓		1.20	10,000		
21		↓	↓	1.30	18,000	↓	↓

Table 3. Full-Scale Store Parameters used in Trajectory

<u>Symbol</u>	<u>GBU-10</u>	<u>MK-84 LDGP</u>	<u>BLU-27B/B(U)</u>
S	1.767	1.767	1.919
b	1.50	1.50	1.563
$\bar{c}$	1.50	1.50	1.563
$I_{xx}$	24.0	16.0	11.5
$I_{yy}$	416.04	360.0	143.0
$I_{zz}$	416.04	360.0	146.0
$C_{mq}$	-275.0	-120.0	-24.0
$C_{nr}$	-275.0	-120.0	-24.0
$C_{lp}$	-20.0	-10.0	0.0
$x_{cg}$	8.042	4.961	5.358
$z_{cg}$	0.0	0.0	0.0
$\bar{m}$	64.0	61.23	24.834
$F_{Z_1}$	4000.0	4000.0	3200.0
$F_{Z_2}$	4000.0	4000.0	2800.0
$x_{L_1}$	0.592	0.666	0.817
$x_{L_2}$	-1.075	-1.000	-0.850
$z_E$	0.342	0.342	0.342

Table 4. Aircraft Loading Configurations



Conf No.	Test Store and Dummies	Left Wing Inb'd Pylon	Centerline Pylon	Right Wing Inb'd Pylon
1	GBU-15 CWW	Empty	Clean	●
2	GBU-15 CWW	●		Empty
3	GBU-15 PWW	Empty		●
4	GBU-15 PWW	●		Empty
5	GBU-8	Empty		●
6	GBU-8	●		Empty
7	GBU-10	Empty		●
8	GBU-10	●		Empty
9	MK-84 LDGP	Empty		●
10	MK-84 LDGP	●		Empty
13	BLU-27 B/B(U)	Empty		●
14	BLU-27 B/B(U)	●	▼	Empty

● Denotes Sting-Mounted Store

○ Denotes Dummy Store

## NOMENCLATURE

BL	Aircraft buttock line from plane of symmetry, in., model scale
b	Store reference dimension, ft, full scale
$C_A$	Store axial-force coefficient, axial force/ $q_\infty S$
$C_\ell$	Store rolling-moment coefficient, rolling moment/ $q_\infty S b$
$C_{\ell_p}$	Store roll-damping derivative, $dC_\ell/d(p b/2V_\infty)$
$C_m$	Store pitching-moment coefficient, referenced to the store cg, pitching moment/ $q_\infty S c$
$C_{m_q}$	Store pitch-damping derivative, $dC_m/d(q b/2V_\infty)$
$C_N$	Store normal-force coefficient, normal force/ $q_\infty S$
$C_n$	Store yawing-moment coefficient, referenced to the store cg, yawing moment/ $q_\infty S b$
$C_{n_r}$	Store yaw-damping derivative, $dC_n/d(r b/2V_\infty)$
$C_Y$	Store side-force coefficient, side force/ $q_\infty S$
DC <sub>j</sub>	Delta coefficient, difference between the measured value of a coefficient at a given point in the grid matrix and the free-stream value of that coefficient at the same attitude
FS	Aircraft fuselage station, in., model scale
$F_{Z_1}$	Forward ejector force, lb
$F_{Z_2}$	Aft ejector force, lb
H	Pressure altitude, ft
$I_{x_x}$	Full-scale moment of inertia about the store $X_B$ axis, slug-ft <sup>2</sup>

$I_{xz}$	Full-scale product of inertia in the store $X_B$ - $Z_B$ plane, slug-ft <sup>2</sup>
$I_{yy}$	Full-scale moment of inertia about the store $Y_B$ axis, slug-ft <sup>2</sup>
$I_{zz}$	Full-scale moment of inertia about the store $Z_B$ axis, slug-ft <sup>2</sup>
$M_\infty$	Free-stream Mach number
$\bar{m}$	Full-scale store mass, slugs
$p$	Store angular velocity about the $X_B$ axis, radians/sec
$p_\infty$	Free-stream static pressure, psfa
$q$	Store angular velocity about the $Y_B$ axis, radians/sec
$q_\infty$	Free-stream dynamic pressure, psf
$r$	Store angular velocity about the $Z_B$ axis, radians/sec
$S$	Store reference area, ft <sup>2</sup> , full scale
$t$	Real trajectory time from initiation of trajectory, sec
$V_\infty$	Free-stream velocity, ft/sec
$WL$	Aircraft waterline from reference horizontal plane, in., model scale
$X$	Separation distance of the store cg parallel to the flight axis system $X_F$ direction, ft, full scale measured from the prelaunch position
$X_{cg}$	Full-scale cg location, ft from nose of store
$X_{L1}$	Forward ejector location relative to the store cg, positive forward of store cg, ft, full scale
$X_{L2}$	Aft ejector location relative to the store cg, positive forward of store cg, ft, full scale

$X_P$	Separation distance of the store cg parallel to the pylon-axis system $X_P$ direction, ft, full scale measured from the prelaunch position
$Y$	Separation distance of the store cg parallel to the flight axis system $Y_F$ direction, ft, full scale measured from the prelaunch position
$Y_P$	Separation distance of the store cg parallel to the pylon-axis system $Y_P$ direction, ft, full scale measured from the prelaunch position
$Z$	Separation distance of the store cg parallel to the flight-axis system $Z_F$ direction, ft, full scale measured from the prelaunch position
$Z_{cg}$	Full-scale cg location, ft, above centerline of store
$Z_E$	Ejector stroke, ft
$Z_P$	Separation distance of the store cg parallel to the pylon-axis system $Z_P$ direction, ft, full scale measured from the prelaunch position
$\alpha$	Aircraft model angle of attack relative to the free-stream velocity vector, deg
$\alpha_s$	Store model angle of attack relative to the free-stream velocity vector, deg
$\beta$	Aircraft model sideslip angle relative to the free-stream velocity vector, deg
$\beta_s$	Store model sideslip angle relative to the free-stream velocity vector, deg
$\theta$	Angle between the store longitudinal axis and its projection in the $X_F$ - $Y_F$ plane, positive when store nose is raised as seen by the pilot, deg
$\Delta\theta$	Angle between the store longitudinal axis and its projection in the $X_P$ - $Y_P$ plane, positive when the store nose is raised as seen by the pilot, deg

- $\phi$  Angle between the store lateral axis and the intersection of the  $Y_B-Z_B$  and  $X_F-Y_F$  planes, positive for clockwise rotation when looking upstream, deg
- $\Delta\phi$  Angle between the store lateral axis and the intersection of the  $Y_B-Z_B$  and  $X_P-Y_P$  planes, positive for clockwise rotation when looking upstream, deg
- $\psi$  Angle between the  $X_F$  axis and the projection of the store longitudinal axis in the  $X_F-Y_F$  plane, positive when the store nose is moved to the right as seen by the pilot, deg
- $\Delta\psi$  Angle between the  $X_P$  axis and the projection of the store longitudinal axis in the  $X_P-Y_P$  plane, positive when the store nose is moved to the right as seen by the pilot, deg

## FLIGHT-AXIS SYSTEM COORDINATES

### Directions

- $X_F$  Parallel to the free-stream wind vector, positive direction is forward as seen by the pilot
- $Y_F$  Perpendicular to the  $X_F$  and  $Z_F$  directions, positive direction is to the right as seen by the pilot
- $Z_F$  Parallel to the aircraft plane of symmetry and perpendicular to the free-stream wind vector, positive direction is downward

The flight-axis system origin is coincident with the aircraft cg and remains fixed with respect to the aircraft during store separation. The  $X_F$ ,  $Y_F$ , and  $Z_F$  coordinate axes do not rotate with respect to the initial flight direction and attitude.

## STORE BODY-AXIS SYSTEM COORDINATES

### Directions

- $X_B$  Parallel to the store longitudinal axis, positive direction is upstream in the prelaunch position

- $Y_B$  Perpendicular to the store longitudinal axis, and parallel to the flight-axis system  $X_F$ - $Y_F$  plane when the store is at zero roll angle, positive direction is to the right looking upstream when the store is at zero yaw and roll angles
- $Z_B$  Perpendicular to both the  $X_B$  and  $Y_B$  axes, positive direction is downward as seen by the pilot when the store is at zero pitch and roll angles

The store body-axis system origin is coincident with the store cg and moves with the store during separation from the airplane. The  $X_B$ ,  $Y_B$ , and  $Z_B$  coordinate axes rotate with the store in pitch, yaw, and roll so that mass moments of inertia about the three axes are not time-varying quantities.

### **PYLON-AXIS SYSTEM COORDINATES**

#### **Directions**

- $X_P$  Parallel to the store longitudinal axis when in the carriage position on the aircraft, positive direction is forward as seen by the pilot
- $Y_P$  Perpendicular to the  $X_P$  axis and parallel to the flight-axis system  $X_F$ - $Y_F$  plane, positive direction is to the right as seen by the pilot
- $Z_P$  Perpendicular to both the  $X_P$  and  $Y_P$  axes, positive direction is downward

The pylon-axis system origin is coincident with the store cg in the prelaunch carriage position. The axes are rotated with respect to the flight-axis system by the prelaunch yaw and pitch angles of the store. Both the origin and the direction of the coordinate axes remain fixed with respect to the flight-axis system throughout the trajectory or survey.